AD-A009 261

PROBLEMS IN LAMINAR FLOW-TURBULENT FLOW

K. M. Case, et al

Stanford Research Institute

Prepared for:

Defense Advanced Research Projects Agency

April 1975

DISTRIBUTED BY:

NTIS

National Technical Information Service
U. S. DEPARTMENT OF COMMERCE

135124

ADA009261

Technical Report JSR-74-2

April 1975

PROBLEMS IN LAMINAR FLOW-TURBULENT FLOW

By: K. M. CASE, A. M. DESPAIN, E. A. FRIEMAN, F. W. PERKINS, J. F. VESECKY

Contract No. DAHC15-73-C-0370
ARPA Order No. 2504
Program Code No. 3K10
Date of Contract: 2 April 1973
Contract Expiration Date: 30 June 1975
Amount of Contract: $1,297,321

Approved for public release; distribution unlimited.

DDC
RECEIVED
MAY 12 1975
D

Sponsored by

DEFENSE ADVANCED RESEARCH PROJECTS AGENCY
ARPA ORDER NO. 2504

STANFORD RESEARCH INSTITUTE
Menlo Park, California 94025 · U.S.A.

Reproduced by
NATIONAL TECHNICAL
INFORMATION SERVICE
US Department of Commerce
Springfield, VA. 22151

Copy No. 8

The views and conclusions contained in this document are those of the authors and should not be interpreted as necessarily representing the official policies, either expressed or implied, of the Defense Advanced Research Projects Agency or the U.S. Government.

80

JASON

SECURITY CLASSIFICATION OF THIS PAGE (When Date Entered)

REPORT DOCUMENTATION PAGE

READ INSTRUCTIONS BEFORE COMPLETING FORM

1. REPORT NUMBER: JSR-74-2

2. GOVT ACCESSION NO.

3. RECIPIENT'S CATALOG NUMBER: AD A009261

4. TITLE (and Subtitle): PROBLEMS IN LAMINAR FLOW-TURBULENT FLOW

5. TYPE OF REPORT & PERIOD COVERED: Technical Report JSR-74-2

6. PERFORMING ORG. REPORT NUMBER: SRI Project 3000

7. AUTHOR(s): K. M. Case A. M. Despain E. A. Frieman F. W. Perkins J. F. Vesecky

8. CONTRACT OR GRANT NUMBER(s): Contract DAHC15-73-C-0370

9. PERFORMING ORGANIZATION NAME AND ADDRESS: Stanford Research Institute, Menlo Park, California 94025

10. PROGRAM ELEMENT, PROJECT, TASK AREA & WORK UNIT NUMBERS

11. CONTROLLING OFFICE NAME AND ADDRESS: Defense Advanced Research Projects Agency, 1400 Wilson Boulevard, Arlington, Virginia 22209

12. REPORT DATE: April 1975

13. NO. OF PAGES: 92

14. MONITORING AGENCY NAME & ADDRESS (if diff. from Controlling Office)

15. SECURITY CLASS. (of this report): UNCLASSIFIED

15a. DECLASSIFICATION/DOWNGRADING SCHEDULE

16. DISTRIBUTION STATEMENT (of this report)

Approved for public release; distribution unlimited.

DDC RECEIVED MAY 12 1975 D

17. DISTRIBUTION STATEMENT (of the abstract entered in Block 20, if different from report)

18. SUPPLEMENTARY NOTES

19. KEY WORDS (Continue on reverse side if necessary and identify by block number)

Transition
Turbulence
Numerical simulation

20. ABSTRACT (Continue on reverse side if necessary and identify by block number)

A program is suggested for the numerical simulation of the transition from laminar to turbulent flow. It is believed that this will materially improve our insight into transition and that it should improve our ability to make predictions. The program is:

- A commitment for 4 to 5 years.
- Parallel calculations (at first) by at least two groups.

(continued)

DD FORM 1 JAN 73 1473
EDITION OF 1 NOV 65 IS OBSOLETE

Reproduced by NATIONAL TECHNICAL INFORMATION SERVICE US Department of Commerce Springfield, VA. 22151

ICATION OF THIS PAGE (When Date Entered)

19. KEY WORDS (Continued)

20 ABSTRACT (Continued)

- The setting up of a small advisory group (approximately 4 members) of active workers in the field who would follow the work closely and provide direction.
- The expenditure of about $200,000 per year.

The problems to be treated (in a preliminary ordering) are:

(1) Transition in the boundary layer over a flat plate,

(2) Transition in the wake of a flat plate,

(3) Transition in the flow over wedges (Falkner-Skan profiles).

(4) Modifications of the flat-plate transition due to suction, roughness, compliant boundary conditions, and heating.

Further problems of interest that might eventually be treated are:

(5) Couette flow between rotating concentric cylinders.

(6) Poiseuille flow between parallel planes.

(7) Poiseuille flow in pipes.

In Appendix A a recommendation is made as to how the best existing techniques for prediction of a transition can be made more generally available. Appendix B addresses the question of a special-purpose Navier-Stokes computer. Appendices C and D are devoted to the problem of boundary conditions.

CONTENTS

ILLUSTRATIONS v

TABLES. vii

I INTRODUCTION 1

II THE FLAT PLATE 5

A. Boundary Conditions 15

B. Calculations at Breakdown 18

III COMPUTER REQUIREMENTS. 19

A. Introduction. 19

B. Finite-Difference Method. 20

C. Spectral Method 20

D. Comparison of Computing Time Estimates. 25

IV WAKE OF A FLAT PLATE 29

V WEDGE FLOWS. 31

VI POSSIBLE FUTURE PROBLEMS 33

A. Couette Flow. 33

B. The Benard Problem. 34

C. Poiseuille Flow 34

D. Modifications of the Flat-Plate Problem 36

VII ON CONTROLLING THE TRANSITION TO TURBULENCE. 37

VIII THE IMPACT OF NUMERICAL SIMULATION OF TURBULENCE 39

IX RECOMMENDATIONS. 41

APPENDICES

A LINEAR-STABILITY ANALYSIS AS A PRACTICAL TOOL 43

B REMARKS ON A SPECIALIZED NAVIER-STOKES COMPUTER . . . 47

C A MODEL TO STUDY DOWNSTREAM BOUNDARY CONDITIONS . . . 59

D BOUNDARY CONDITIONS 65

E THREE-DIMENSIONAL IN-PLACE FAST-FOURIER TRANSFORM ARRAY 77

REFERENCES 83

ILLUSTRATIONS

1	Measured Velocity Distribution in the Laminar Boundary Layer on a Flat Plate at Zero Incidence.	6
2	Curve of Neutral Stability for the Wavelengths $\alpha\delta^*$ of the Disturbances in Terms of the Reynolds Number R for the Boundary Layer on a Flat Plate at Zero Incidence (Blasius Profile)	10
3	Curve of Neutral Stability for the Frequency β_r of the Disturbances and Wave Propagation Velocity c_r for the Boundary Layer on a Flat Plate at Zero Incidence (Blasius Profile)	11
4	Variation of Amplitude of the u'-Fluctuation for Two Neutral Disturbances in a Laminar Boundary Layer on Flat Plate at Zero Incidence.	12
5	Distribution of Intensity of u-Fluctuation Across Boundary Layer: 145-c/s Wave, $U_1/\nu = 3.1 \times 10^5$ ft^{-1}.	13
6	Geometry of Flat-Plate Navier-Stokes Problem	19
7	The Form of the Neutral Curve in the (k,Re) Plane for a Plane Poiseuille Flow.	35
D-1	Coordinate System.	69
D-2	Stability Diagram for Boundary-Layer Flow.	73
E-1	Perfect Shuffle Connections for 1-D FFT, N = 16.	81
E-2	4-by-4 Array of Cells for a 2-D FFT Network.	81

TABLES

1	Three-Dimensional Finite-Difference Technique	21
2	Estimated Computing Time for Spectral and Finite-Difference Methods.	26
B-1	Parameters of an Interesting Turbulence Calculation . . .	50
B-2	Maximum-Performance Parameters for a Modern Single, Pipelined and Cashe CPU Computer.	51
B-3	ILLIAC IV Parameters.	52
B-4	Cellular-Array-Computer Parameters.	56

1 INTRODUCTION

It is clear that a fundamental understanding of turbulence would be of great practical significance. Since it is suspected that on the very smallest scales turbulence has certain universal features, it might be hoped that these would be revealed by a direct numerical simulation. Unfortunately the problem of fully developed turbulence is one involving very many degrees of freedom. Indeed, if R is the Reynolds number, the necessary degrees of freedom to be treated in a given dimension are of the order of $R^{3/4}$. In three dimensions this number is then of the order of $R^{9/4}$ (see, for example, Landau and Lifshitz, 1959: for more detailed estimates, see Case et al., 1973).* Since time steps are restricted by space steps, the number of needed calculations then grows as R^3 (Case et al., 1973). For the large values of R occurring in practice the computations then become prohibitive with present (or soon-to-be-available) computers.

Under these circumstances it is perhaps reasonable to back off a bit and ask what can be done in the way of a numerical investigation of the transition from laminar to turbulent flow. Here, unless otherwise indicated, we restrict ourselves for simplicity to the incompressible case--i.e., our flows are described by the Navier-Stokes equations

$$\frac{\partial \underset{\sim}{v}}{\partial t} + \underset{\sim}{v} \cdot \nabla \underset{\sim}{v} = -\nabla P + \nu \nabla^2 \underset{\sim}{v} \qquad (1)$$

$$\nabla \cdot \underset{\sim}{v} = 0 \quad . \qquad (2)$$

---

*References are listed at the end of the report.

Knowledge of such transitions also has considerable significance for practical designs. The hope is that we will be able to treat such problems with presently available computers, since:

(1) Transition frequently takes place at relatively low Reynolds number.

(2) Transitions are frequently seen to develop through a number of stages in which the flow is relatively large-scale (i.e., involving relatively few degrees of freedom).

Experimentally, the transition takes place in many different ways. Indeed, for a given practical situation more than one mechanism may be responsible. There are a number of ways in which one can characterize the different possibilities. None of these is completely satisfactory in that the descriptions are not necessarily unique or mutually exclusive. One such cataloging is in terms of whether the transition occurs in a flow that is inviscidly stable or not. Another rather convenient distinction is between transitions in "free" or "bound" boundary layers (Sato and Kuriki, 1961). In essence, the difference is between flows that become turbulent rapidly and those that become turbulent gradually. It is the latter class that we expect to be most amenable to numerical simulation. However, as we will see, the division is by no means sharp.

Accordingly, we consider the calculation of transition in a variety of simple situations that have shown different forms of transition. We start with problems in which there is much detailed experimental information available and some theoretical insight. As will be seen, this knowledge is very useful in showing us what size calculation must be performed and what one expects to be able to describe. Assuming that the initial calculations are successful, we then indicate others that can be done that hopefully will lead to methods, in which there is confidence, for calculating transition in situations of practical interest.

Our program is then as follows. First we consider various situations in which transition could be calculated. These are enumerated essentially in the order of what we consider their priority. In each case we describe the physics of the situation and our present understanding. In various degrees of detail we discuss the limitations of the calculations (resolution needed and uncertainties). An estimate is then made of the computation effort required. Second, we give some recommendations as to how a program to do these things could be implemented. These include cost per year, number of years, organization, and supervision.

It is felt certain that such a program would contribute significantly to the present state of the art with a relatively modest expenditure of funds. It is hoped this will lead to a capability of doing some practical calculations.

II THE FLAT PLATE

As a first calculation we suggest the numerical study of the transition in the boundary layer in the flow over a flat plate. The advantages of this are:

(1) Codes ior this have been developed and some calculations have been performed (Grosch, 1974; Orszag, 1974).

(2) Excellent detailed experimental information is available (Klebanoff et al., 1961; Kovasznay et al., 1962).

(3) Considerable theoretical insight is available. Thus the initial stage of laminar instability is well understood (Schlichting, 1960). Theoretical models give a qualitative picture of what happens in the later stages (e.g., Benny, 1961; Stuart, 1962; Lin and Benny, 1962; Greenspan and Benny, 1963).

There are also disadvantages:

(1) As indicated in our earlier report (cf. Schlichting, 1960, p. 386) there are some ambiguities concerning downstream boundary conditions.

(2) At the last stages before complete turbulence is obtained, small-scale motions are found. There is some question as to whether a calculation designed to follow the earlier stages of transition can resolve these.

We return to these two points later.

To illustrate what is involved in the calculation of transition of the boundary-layer flow over a flat plate, we give a brief (and idealized) version of the experiment described by Klebanoff et al. (1961).

Over a flat plate located at $x \geq 0$, $y = 0$ there flows a fluid with velocity U_∞ in the x direction toward the plate. The pressure gradient

Preceding page blank

is adjusted to be zero. A ribbon is located above the plate in a spanwise (z) direction perpendicular to the flow at some distance downstream from the leading edge. Under the ribbon there are strips uniform in length and uniformly separated. With the ribbon stationary the x component (u) of the velocity is, for any x and z, as shown in Figure 1.

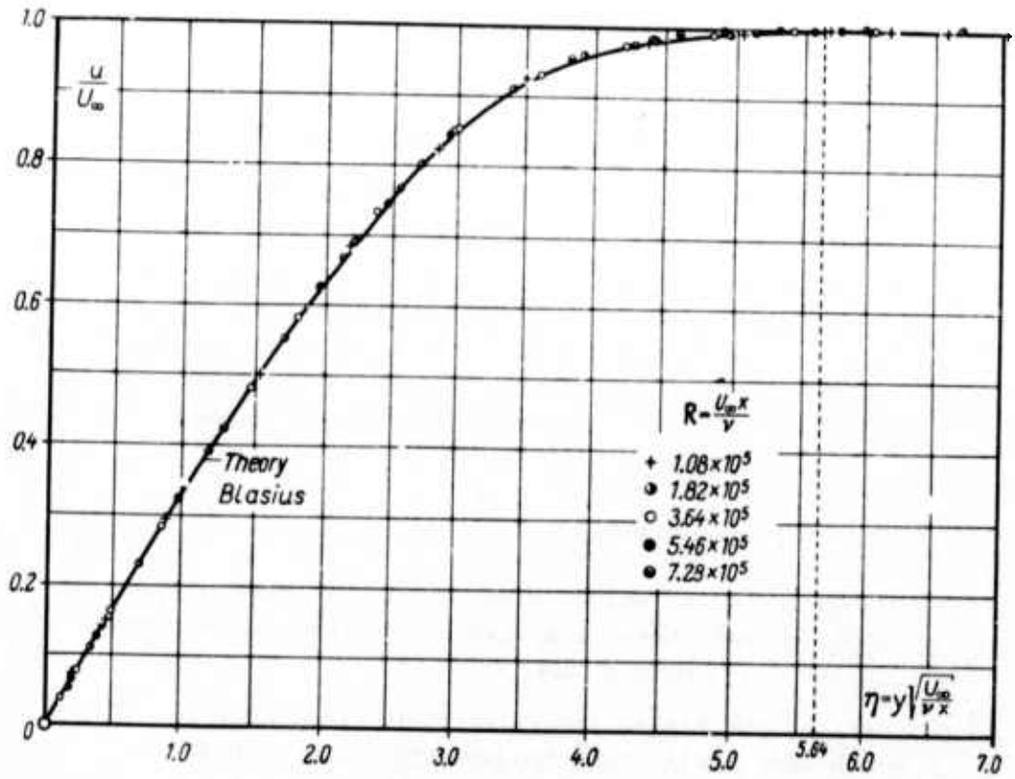

FIGURE 1 MEASURED VELOCITY DISTRIBUTION IN THE LAMINAR BOUNDARY LAYER ON A FLAT PLATE AT ZERO INCIDENCE. Source: Schlichting (1960).

The ribbon is then vibrated at a frequency f. At small amplitudes of oscillation the results are as follows. For a fixed distance x downstream the velocity varies essentially sinusoidally in time and with wavelength, which is the periodicity of the strips in the z direction. The average velocity distribution as a function of y retains essentially the form of Figure 1. As we go downstream the amplitude of the oscillations in u first increases and then gradually decreases.

At a larger amplitude of oscillation the picture changes. As we proceed downstream from the ribbon the situation is first as above. Further down, however, there develops a pronounced three-dimensional structure characterized by large spanwise variations in wave amplitude with "peaks" and "valleys" occupying fixed spanwise positions. Associated with this variation in amplitude there is also a spanwise variation in local mean velocity such that there is a defect at a peak and an excess at a valley. Further downstream there occurs an abrupt increase in amplitude at a peak that is characterized by a series of intense low-velocity pulses--evidenced by "spikes" in an oscillogram of streamwise fluctuating velocity. At first a single spike appears for each cycle of the primary oscillation. The spikes increase in number as we go downstream and ultimately blend into fully developed turbulence.

Present theoretical understanding is the following. In the absence of the vibrating ribbon the stationary laminar flow is adequately described by the boundary-layer equations for the velocity $[u(x,y), v(x,y), w = 0]$:

$$\frac{u\partial u}{\partial x} + \frac{v\partial u}{\partial y} = \nu \frac{\partial^2 u}{\partial y^2} \tag{3a}$$

$$\frac{\partial u}{\partial x} + \frac{\partial v}{\partial y} = 0 \quad , \tag{3b}$$

$$u = v = 0 \text{ at } y = 0 \quad , \quad \lim_{y\to\infty} u = U_\infty \quad .$$

These equations have the Blasius similarity solution

$$u = U_\infty f(\eta) \quad , \quad v = \sqrt{\frac{U_\infty \nu}{x}}\, f_1(\eta) \tag{4}$$

where

$$\eta = y\sqrt{\frac{U_\infty}{\nu x}}$$

With

$$f(\eta) = \varphi'(\eta) \quad , \quad f_1(\eta) = 1/2[\eta\varphi'(\eta) - \varphi]$$

we have

$$\varphi\varphi'' + 2\varphi''' = 0 \tag{5}$$

subject to

$$\varphi(0) = \varphi'(0) = 0 \quad , \quad \varphi'(\infty) = 1 \quad .$$

Numerical integration then gives the velocity profile of Figure 1--in excellent agreement with experiment.

Remarks:

(1) Two conventional measures of the boundary-layer thickness used are:

(a) δ = that value of y for which $u = 0.99U_\infty$. Numerically,

$$\delta \approx 5\sqrt{\frac{\nu x}{U_\infty}} \quad . \tag{6}$$

(b) $$\delta^* = \int_0^\infty \left(1 - \frac{u}{V_\infty}\right) dy \approx 1.73\sqrt{\frac{\nu x}{U_\infty}} \quad .$$

(2) For the experiment of Klebanoff et al. (1961) approximate numbers are $U_\infty \sim 1500$ cm/s, $\nu = 0.15$ cm^2/s, and $x_{ribbon} \sim 100$ cm. Then, $\delta_{ribbon} \sim 0.5$ cm. Typically

the variations described above occurred within 40 cm of the ribbon. At this point δ has changed by only ~20%.

(3) From Figure 1 and the above we conclude:

(a) The velocity distribution varies smoothly within the boundary layer.

(b) After but a few δ from the plate (~1 cm for the experiment) the flow is essentially arbitrarily close to the free-stream velocity.

To study the effect of external disturbances it is natural to turn to linear stability theory. Thus, in Eqs. (1) and (2) we substitute

$$\underset{\sim}{u} = \underset{\sim}{u}_o + \delta\underset{\sim}{u} \tag{7}$$

where $\underset{\sim}{u}_o$ is the original laminar flow, and we retain only terms linear in the perturbation $\delta\underset{\sim}{u}$. Assuming that a time dependence $\delta\underset{\sim}{u} \sim e^{-i\omega t}$ leads to an eigenvalue problem. If it is found that $\text{Im}\ \omega \equiv \omega_i$ is > 0, then initial perturbations can grow, and we have instability. In practice, another approximation is made. Stability <u>locally</u> is studied by assuming that the profile (y dependence) is such that the one at a given position x_o really extends from $-\infty < x < \infty$. (Since in the problems considered here the true x variation of the profile is very slow, this is a readily justifiable approximation). In this case the eigenvalue problem is simplified. Since there is no explicit x-dependence we can limit ourselves to investigating solutions with x and z dependence of the form $\sim e^{-(\alpha x+\beta z)}$. [Since Squire's theorem (Schlichting, 1960, p. 386) assures us that the onset of instability occurs first when $\beta = 0$, the original solutions of the eigenvalue problem were obtained for this case]. With this form of x-dependence the eigenvalue problem can be regarded as one in which α is given (real) and the complex ω is sought.

Figure 2 gives the results for an old calculation of the curve for neutral stability in the $\alpha\delta^*$, $R_{\delta^*} = U_\infty\delta^*/\nu$ plane. It may be noted that

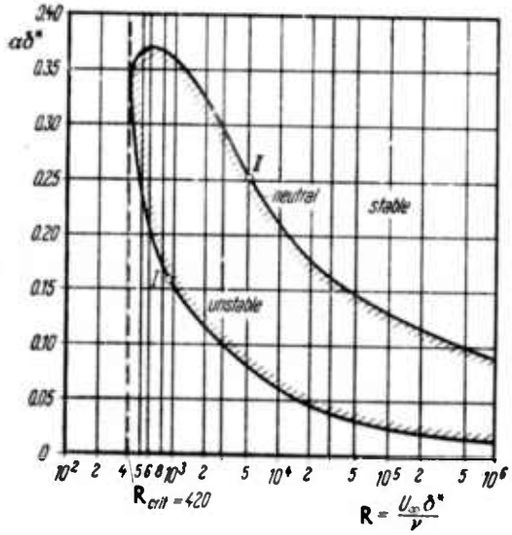

FIGURE 2 CURVE OF NEUTRAL STABILITY FOR THE WAVELENGTHS $\alpha\delta^*$ OF THE DISTURBANCES IN TERMS OF THE REYNOLDS NUMBER R FOR THE BOUNDARY LAYER ON A FLAT PLATE AT ZERO INCIDENCE (Blasius Profile). Source: Schlichting (1960).

for instability, $R_{\delta *}$ must be greater than a critical value $R_{\delta *c} \sim 500$ and $\alpha\delta^*$ must be less than about 0.36 (i.e., there is a minimum wavelength $\lambda_{min} \sim 2\pi\delta^*/0.36 \sim 17.5\delta^* \sim 6\delta$ for instability). For the experiment described above this wavelength is $\lambda_{min} \sim 3$ cm, while the distance x_c downstream from the leading edge where instability can possibly occur is $x_c \sim 80$ cm.

For the experiment, however, it is somewhat more relevant to consider a real ω and find the, in general, complex α. (With $\alpha_i = \text{Im}\,\alpha < 0$, we have spatial amplification.) A neutral curve in the ω, $R_{\delta *}$ plane is shown in Figure 3. We see that there is a maximum frequency for which such spatial amplification holds. This is

$$\frac{\omega_{max}\,\delta^*}{U_\infty} \sim 0.19 \quad .$$

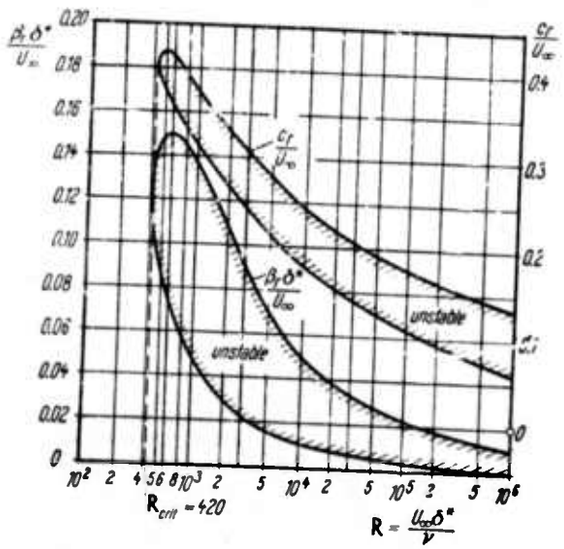

FIGURE 3 CURVE OF NEUTRAL STABILITY FOR THE FREQUENCY β_r OF THE DISTURBANCES AND WAVE PROPAGATION VELOCITY c_r FOR THE BOUNDARY LAYER ON A FLAT PLATE AT ZERO INCIDENCE (Blasius Profile). Source: Schlichting (1960).

For the experiment described, this is:

$$f_{max} \sim 300 \text{ c/s} \quad .$$

We note also from Figure 3 that the phase velocity ($c_r = \omega/\alpha$) of the neutral waves is of order $0.4U_\infty$ or less.

The theoretical picture of the early stages of the experiment described is then the following. The oscillating ribbon excites waves of wavelength $\lambda \gtrsim 3$ cm. These are then amplified as we go downstream. If the initial perturbation is sufficiently small we will pass through the right-hand neutral curve before the amplitudes are large enough to void the linear assumption. As we go farther downstream the disturbance will then be damped out. On the other hand, if the initial disturbance is large enough it will be amplified within the unstable region downstream to a point where linear-stability theory no longer applies and cannot be used for prediction.

One further result of linear-stability theory of importance for us is the shape of the eigenfunctions corresponding to the unstable mode. From Figure 4 we see that they vary rapidly in the part of the boundary layer between y = 0 and y = 0.2 - 0.4δ. (For the experiment, this number is y = 0.1 - 0.2 cm.) Outside this region the variation is rather smooth.

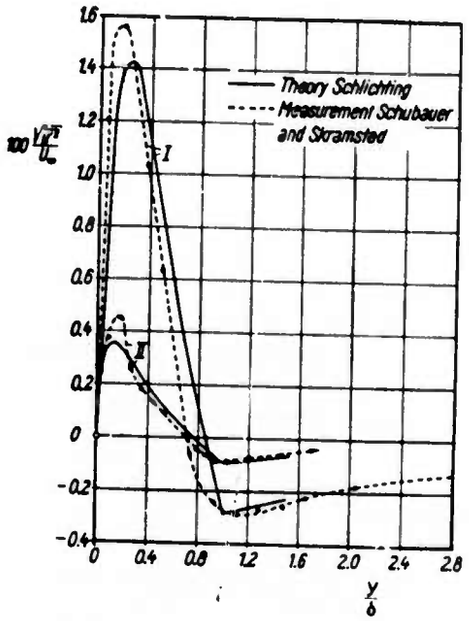

FIGURE 4 VARIATION OF AMPLITUDE OF THE u'-FLUCTUATION FOR TWO NEUTRAL DISTURBANCES IN A LAMINAR BOUNDARY LAYER ON FLAT PLATE AT ZERO INCIDENCE. The curves labeled I and II correspond to the two neutral disturbances I and II in Figure 2. Source: Schlichting (1960).

The further development of the flow toward turbulence is somewhat less known theoretically. From models (Benny, 1961; Stuart, 1962; Lin and Benny, 1962; Greenspan, 1962; Greenspan and Benny, 1963) and experiment (Klebanoff et al., 1961) it appears that the amplified two-dimensional Tollmien-Schlichting wave interacts, as a result of nonlinear terms, with true 3-dimensional disturbances produced by the spacers. This combination then gives rise to the distorted boundary layer which in turn results in the production of the high-frequency disturbances. While

the primary contribution of a numerical simulation would be to allow the development of the nonlinear interaction, two qualitative conclusions can be drawn:

(1) Resolution in the spanwise (z) direction must be sufficient so that the expected peaks and valleys can be adequately differentiated.

(2) While the Tollmien-Schlichting waves have their largest amplitudes and sharpest variation close to the plate (~0.1δ) the fluctuations near breakdown have their largest values much farther out (~0.5δ)-- cf. Figure 5. From this we conclude that even at these distances the resolution cannot be too coarse.

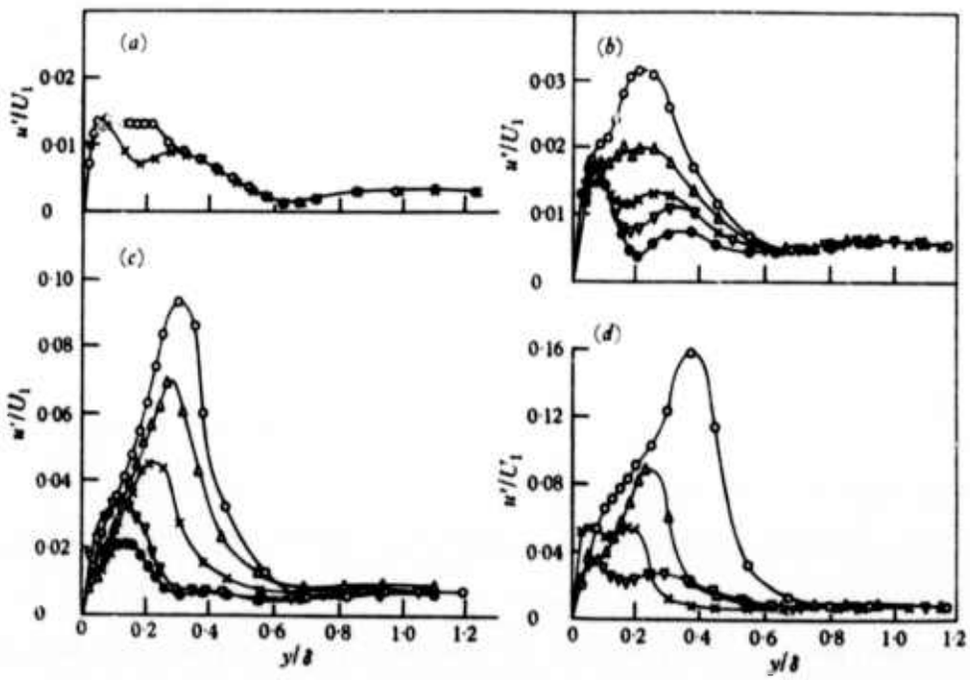

FIGURE 5 DISTRIBUTION OF INTENSITY OF u-FLUCTUATION ACROSS BOUNDARY LAYER: 145-c/s WAVE, $U_1/\nu = 3.1 \times 10^5$ ft^{-1}. Source: Klebanoff et al. (1961).

Let us now turn to the numerical simulation of the above experiment. Clearly, finite computer capacity restricts us to a discussion of the flow to some finite region of space and time. In the x (streamwise) direction this should begin somewhat downstream from the leading edge of

the plate to assure the initial establishment of the laminar flow, but upstream from the ribbon to diminish spurious effects due to incorrect boundary conditions. A reasonable guess would be to start at a position $(2\text{-}5)\lambda_{min}$ upstream from the ribbon (where λ_{min} is the minimum unstable Tollmien-Schlichting wavelength). Downstream from the ribbon we would like to include all positions till the onset of turbulence. Experimentally this is $\sim 6\lambda_{min}$. However, as indicated, later ambiguities in the boundary conditions suggest that the end position be chosen as far downstream as feasible. A compromise might be that the region in x to be described is of the order of $(10\text{-}20)\lambda_{min}$. Since in the spanwise (z) direction we are describing a periodic behavior, we can restrict ourselves to a distance equal to one wavelength of the spanwise perturbation. In the direction perpendicular to the plate we can, since the laminar flow and its perturbations go to zero rapidly outside the boundary-layer thickness δ, restrict ourselves to a distance of a few δ (say, 2δ). In time we would like to follow the flow for some significant number of oscillations. If T be the period of the ribbon the time of interest may be of the order of (5-10)T.

Now what do these dimensions imply about the number of calculations to be performed? The problem is to solve Eqs. (1) and (2) in the region described, subject to suitable boundary conditions (discussed below). To estimate, we imagine the calculation done by finite-difference methods in all dimensions. (If spectral methods are used, a rule of thumb might be that the number of modes in a given direction be $\sim(1/2 \rightarrow 1/3)$ of the number of grid points. In the x-direction we want to describe a distance of the order $15\lambda_{min}$. Assuming that this is adequately resolved by 8 points per wavelength we have something like 160 points in the x-direction--i.e., in the notation below, $L \sim 160$. In the z-direction we have a distance of only one perturbation wavelength, but to have a chance of describing the variation near breakdown we need a fine resolution. A

guess is 16 points in this direction (N = 16). In the δ-direction we have a total distance 2δ, but as we have seen in the region $0 \leq y \lesssim 0.2\delta$, there are very rapid variations. Hence, with finite-difference methods one would use either some coordinate mapping or a varying grid size. Assuming the latter, one might use of the order of 20 points for the first 0.3δ and 20 more for the remainder--i.e., of the order of 40 grid points. The sizes of the time steps are essentially determined by stability requirements--i.e.,

$$\bar{v}\Delta t < \Delta \underset{\sim}{r}$$

where $\bar{v}$ is some appropriate velocity and Δr is some mesh spacing. Since U_∞ is the largest velocity and it is in the x-direction, a reasonable criterion (Grosch, 1974) might be

$$\Delta t \lesssim \frac{\Delta x}{U_\infty} \quad .$$

With the numbers suggested above, this is

$$\Delta t \lesssim \frac{0.375}{1.5 \times 10^3} \sim 2.5 \times 10^{-4}$$

For $T = 1/150$ c/s $= 6.7 \times 10^{-3}$, this implies of the order of 30 time steps per cycle and therefore a number of time steps $N\hat{t} \sim 300$ to 500.

Computer requirements based on these numbers are discussed below. First, however, we include a few caveats.

A. Boundary Conditions

A well posed problem for solutions of Eqs. (1) and (2) would be one in which the initial velocity is prescribed everywhere within the region described and the velocity is given everywhere on the boundary

for all time (subject to $\int_S \underset{\sim}{n} \cdot \underset{\sim}{u}\, ds = 0$). Unfortunately we do not know this information. At $y = 0$ we do. There all components of the velocity are zero. At $y = 2\delta$ it is clearly correct to a very high degree of approximation to take the velocity as that of the free stream. At the upstream edge of our region it is reasonable to assume that the velocity is of the Blasius form plus whatever perturbation one might want to put in. In the spanwise direction a periodicity requirement is reasonable. What we do not know is the velocity at the downstream edge of our region. Two somewhat ad hoc suggestions have been made. Grosch (1974) suggests "extrapolating" from the velocity inside. If L is the downstream edge of the region, this formally is of the form

$$u(L,y,z,t) = \int_0^L u(x,y,z,t)\, g(x)\, dx + \int_0^L \frac{\partial u}{\partial t}(x,y,z,t)\, h(x)\, dx \quad .$$

In some sense this may be regarded as a kind of radiation condition, which might indeed be reasonable. How well the actual choice made of $g(x)$ and $h(x)$ approximates such a condition is not clear. Also, there is an uncomfortable situation in that the pressure at $x = L$ is calculated from $\partial u/\partial t$, while to advance forward in time $\partial u/\partial t$ is calculated using the resulting p. The possibility of an instability occurs.

Orszag (1974) proceeds by dropping certain terms as small. With the emasculated equations he demonstrates uniqueness if at all boundary points either p or $\underset{\sim}{v} \cdot \underset{\sim}{n}$ is given as well as $\underset{\sim}{v}$ for points such that $\underset{\sim}{v} \cdot \underset{\sim}{n}_{out} < 0$. (Note: this demonstration involves an additional, but reasonable, approximation.) The difficulties here are:

(1) We do not know p or $\underset{\sim}{v} \cdot \underset{\sim}{n}$ on the downstream boundary.

(2) We do not know $\underset{\sim}{v}$ so that we cannot even determine when $\underset{\sim}{v} \cdot \underset{\sim}{n}_{out} < 0$.

(3) The approximations involved need to be justified. (In fairness it must be noted that Orszag has recently

suggested some modified boundary conditions about which we have insufficient information to permit making an evaluation.)

We would like to suggest that results obtained will be rather insensitive to the choice of downstream boundary conditions. There are two arguments:

(1) For Tollmien-Schlichting waves the group velocity (c_g) is of order $1/3U_\infty$. Here then $c_g \sim 500$ cm/s. Then to travel a distance of the order of 50 cm from the ribbon to the downstream edge requires $\sim 1/10$ s, which is approximately 15 periods of oscillations, and one might not even follow the developments much further in time.

(2) The essential use of the velocity on the boundary is to compute the pressure within our region. This can be obtained by taking a special solution of the Poisson equation and adding to it a solution of Laplace's equation

$$\nabla^2 P = 0$$

chosen to satisfy the boundary condition. If the y variation of the boundary condition is $\sim e^{iky}$, then the fall-off in the x direction is:

$$P \sim P_o e^{-k|x-L|} \quad .$$

Now a reasonable guess for the y variation is $k2\delta \sim 2\pi$. (Remark: We are thinking of deviations from the Blasius profile. For the latter, of course, P is independent of y.) This suggests, then, that the boundary conditions imposed at the downstream edge will have little effect a few wavelengths upstream. It is for this reason that we have suggested that the downstream edge of the calculation region be some distance beyond where we hope to find a turbulent transition.

A further argument that suggests things are insensitive to the downstream boundary conditions is found by noting that the velocities (phase and group) of the Tollmein-Schlichting waves are usually small ($\sim 1/3$)

compared to the free-stream velocity. This suggests that any such disturbance will be convected downstream and have little effect upstream.

In Appendix C we give a simple model for which the arguments for exponential fall-off and downstream convection are verified in detail.

However, it is obvious that none of the above arguments are rigorous. It is essential that whatever boundary conditions are used should be varied (within reasonable limits) to see how far upstream we need to be in order to have confidence that the results are not artifacts caused by the assumptions made.

B. Calculations at Breakdown

As we have noted, there comes a point where the boundary layer is so modified by the nonlinear wave interactions that it becomes strongly unstable. At this point high-frequency oscillations suddenly appear. In model calculations the instabilities grow by orders of magnitude in a fraction (~ 1/10) of the primary period. The scheme described above will not be able to follow such rapid variations. At best, a large irregular change in velocities between two successive time steps might be found. However, even this may not occur--the large space and time differences may average out such irregularities. One approach to proceeding further is suggested by the fact that breakdown (Klebanoff et al., 1961) appears to occur at very localized points. Hence, we can stop the calculation when at some x,z there is a profile that according to linear stability theory is highly unstable. Then we consider only a small region in the vicinity of this point. For this region we introduce a much smaller space-time mesh and then integrate the Navier-Stokes equation with initial conditions obtained from the previous calculation.

III COMPUTER REQUIREMENTS

A. Introduction

The basic problem under consideration is that of flow over a flat plate as illustrated in Figure 6. L, M, and N are the numbers of mesh

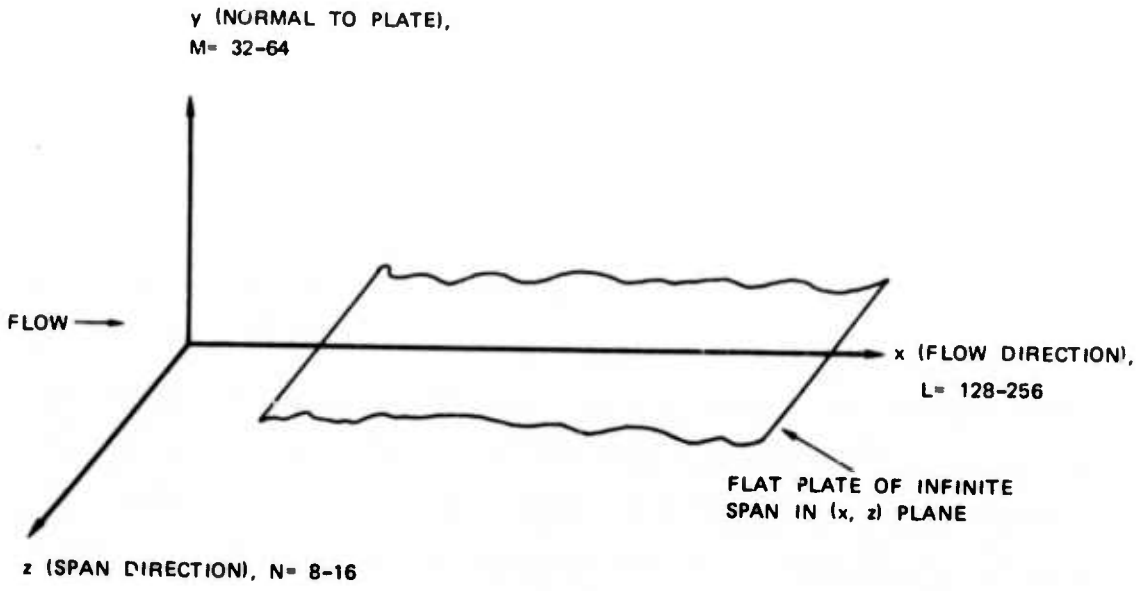

FIGURE 6 GEOMETRY OF FLAT-PLATE NAVIER-STOKES PROBLEM

points in the x, y, and z directions at which one calculates the flow variables $\underset{\sim}{v}$ and P. Two approaches to the solution of the Navier-Stokes equations on digital computers are considered here: the finite-difference scheme of Dr. Chester Grosch, and the spectral method of Dr. Steve Orszag. We have examined the finite-difference method in considerable detail with the help of Dr. Grosch, but the spectral method has proved more difficult to investigate, as noted below. The objective of this section is to make some computer-run-time estimates for both methods on three-dimensional problems of interest. The results should not be taken as a

comparison of the two methods (as we discuss below), but rather as an indication of the computer run time and therefore cost that one can expect on optimized "production runs" for useful problems.

B. Finite-Difference Method

The finite-difference method for flow over a flat plate in two dimensions (x,y) is discussed in detail by Grosch (1974). The method is fairly easily generalized to three dimensions. The basic changes are that the Poisson equation for the pressure $\nabla^2 P - Q = 0$ must be solved in three dimensions and that three components of v are required, thus complicating the finite-difference equations. The Poisson equation is solved by taking a two-dimensional Fourier transform in the (x,z) plane for each of the M values of y in the mesh. We then solve (LN) tridiagonal equation systems--i.e., one system for each mesh point in the (x,z) plane. This solution yields the Fourier components of P for each plane perpendicular to the y axis. An inverse Fourier transfrom then yields P. A set of three finite-difference equations yields the three components of $\underset{\sim}{v}$ and the loop is completed. Table 1 summarizes the operations required and the total number of operations per time step. Multiplying the terms in Table 1 by their appropriate computation times yields the total computer time (ΔT_{fd}) per calculation time step:

$$\Delta T_{fd} \approx LMN \left\{ t_a (95 + 3 \log_2 LN) + t_m (81 + 2 \log_2 LN) + 28 t_s \right\} \qquad (8)$$

where t_a, t_m, and t_s are the particular computer's add, multiply, and memory access times.

C. Spectral Method

It is impossible to determine exactly how Orszag implemented his calculation. If his report (Orszag, 1974) is examined it will be

Table 1

THREE-DIMENSIONAL FINITE-DIFFERENCE TECHNIQUE

	Additions	Multiplications	Memory Transfers
1. Pressure Calculation Solving $\nabla^2 P - Q = 0$ in Three Dimensions			
A. 2-D Fourier transform of $[Q_{i,j}]$ M times	1.5 LMN $\log_2$LN	LMN $\log_2$LN	2 LMN
B. Tri-diagonal equation systems of size M solved (LN) times	10 LMN	3 LMN	5 LMN
C. 2-D Fourier transform to obtain $[P_{i,j}]$ M times	1.5 LMN $\log_2$LN	LMN $\log_2$LN	2 LMN
2. Finite-Difference Calculation of Three Components of $\underset{\sim}{v}$	85 LMN	78 LMN	19 LMN
Total operations per time step	LMN(95 + 3 $\log_2$LN)	LMN(81 + 2 $\log_2$LN)	28 LMN

Source: C. E. Grosch.

noticed that no detailed discussion is given about the solution technique. Verbal conversations with Orszag helped some, but it is difficult to judge the validity and efficiency of the calculations. In at least one case, the report contains conflicting statements concerning the step-integration method employed. "Adams-Bashforth" is indicated on p. 31, but "Runge-Kutta" is used in the actual code. Since the computer code still contains "bugs," it is not clear just how valuable the results of the study were. Although it is not evident from the report, it is absolutely true that Orszag has made significant contributions to the field.

The general method can be described as a part spectral method and part finite-difference method. According to Orszag, 20 two-dimensional real FFTs (fast Fourier transforms) and two one-dimensional FFTs are required for each plane normal to the flow per time step, and the time spent in FFTs is 60% of the total computer run time. Also, he stated that it took 9 seconds per time step for L = 128, M = 8, and N = 64. Thus, a general formula for estimating the run time on a CDC-7600 can be derived as follows.

First, let us consider FFT operations:

(1) Complex transform in one dimension requires

$\left(\frac{N}{2}\right) \log_2 (N)$ butterflies with

4 multiplies + 2 additions/rotation + 4 additions/butterfly

= multiplies + 6 additions for each butterfly yielding

$3N \log_2(N)$ additions and

$2N \log_2(N)$ multiplications in all.

(2) Real transform in one dimension requires

$\left(\frac{N}{4}\right)\left[\log_2 \left(\frac{N}{2}\right) + 1\right]$ butterflies or

$$N\left[\log_2\left(\frac{N}{2}\right) + 1\right] \cong N \log_2 N \text{ multiplications and}$$

$$\left(\frac{3N}{2}\right) \log_2 N \text{ additions.}$$

(3) 2-D complex transform (M × N) requires

$$M\left[\frac{N}{2} \log_2 (N)\right] \text{ butterflies (1-D Transforms)}$$

followed by

$$N\left[\frac{M}{2} \log_2 M\right] \text{ butterflies (1-D Transforms)}$$

$$= \frac{NM}{2}\left[\log_2 M + \log_2 N\right] = NM \log_2 MN \text{ butterflies}$$

or

$$NM \log_2 (MN) \times \begin{cases} 4 \text{ multiplication} \\ 6 \text{ addition} \end{cases}$$

$$= \begin{cases} 4\ MN \log_2 (MN) \text{ multiplications} \\ 6\ MN \log_2 (MN) \text{ addition.} \end{cases}$$

(4) 2-D real transform (M × N) requires

$$M\left\{\frac{N}{4}\left[\log_2\left(\frac{N}{2}\right) + 1\right]\right\} \text{ butterflies followed by}$$

$$N\left\{\frac{M}{4}\left[\log_2\left(\frac{M}{2}\right) + 1\right]\right\} \text{ butterflies}$$

$$= \frac{MN}{4}\left[\log_2\left(\frac{M}{2}\right) + \log_2\left(\frac{N}{2}\right) + 2\right] \approx \left(\frac{MN}{4}\right) \log_2 MN \text{ butterflies}$$

or

$$+ \begin{cases} MN \log_2 MN \text{ multiplies} \\ \frac{3MN}{2} \log_2 MN \text{ additions} \end{cases} .$$

Orszag has estimated that the (20L) two-dimensional real FFTs and (2L) one-dimensional FFTs require about 60% of his computing time. For the 7600, multiplication is about twice the time of an addition. Define one operation as an addition; hence, multiplication is equivalent to two operations and a butterfly is 14 operations:

$$2L \text{ (1D FFTs)} \approx 14L \left[\left(\frac{M}{4}\right) \log_2 M + \left(\frac{N}{4}\right) \log_2 N \right] \text{ operations}$$

$$20L \text{ (2D FFTs)} \approx 20 \times 14L \left(\frac{MN}{4}\right) \log_2 (MN) \text{ operations} \quad .$$

The total run time (ΔT_s) per computation time step on the 7600 is then

$$\Delta T_s \approx K' \left(\frac{1}{0.6}\right) (14L) \left[5 \text{ MN } \log_2 (MN) + \left(\frac{M}{4}\right) \log_2 M + \left(\frac{N}{4}\right) \log_2 N \right]$$

$$\Delta T_s \approx K'L \left[117 \text{ MN } \log_2 (MN) + 5.8 \text{ M log M} + 5.8 \text{ N log N} \right]$$

where K' is a calibration factor (equal to the add time in seconds). Now, from Orszag's experience on the 7600 we know that $\Delta T_s \approx 9s$ for L = 128, M = 8, and N = 64. Substituting this into the above equation yields $K' \approx 1.3 \times 10^{-7}$, so the effective add time (t_s) is about one μs.

Now, for a single-calculation time step we will allow 60% of the run time to the 20L two-dimensional FFTs--i.e., neglecting the two one-dimensional FFTs, we allow 30% of the run time to the solution of tri-diagonal equation systems, and 10% of the run time to 14 memory accesses per mesh point. So from Orszag's experience we can derive an approximate formula giving ΔT_s, the computing time required for a single time step in the Navier-Stokes calculation:

$$\Delta T_s \approx LMNt_a \text{ (45 } \log_2 MN) + LMNt_m \text{ (30 } \log_2 MN) + 14 \text{ LMN} t_s \qquad (9)$$

where L, M, and N are the numbers of mesh points in the x (flow), y (normal), and z (span) directions; and t_a, t_m, and t_s are the computer's effective addition, multiplication, and memory access times.

D. Comparison of Computing Time Estimates

The computing-time estimates (per time step) for the finite difference and spectral methods discussed above are given by Eqs. (8) and (9). The particular computer's effective add, multiply, and memory access times are denoted by t_a, t_m, and t_s. Two features are common to both methods:

(1) The computing time increases approximately linearly with the number of mesh points.

(2) The multiplication terms are more heavily weighted than the addition terms when one considers that multiply times are typically about twice as long as add times.

However, there are also some interesting differences. The finite-difference method is more sensitive to memory access time and therefore will fare relatively worse on a memory-limited machine. For a typical application the spectral method is most heavily governed by the multiplication time, while the finite-difference method is about equally dependent on the multiplication and memory access times.

The computing-time estimates given below should be qualified on several points. First, the estimates are intended only as a very rough guide to the sort of computing times one might expect on rather highly optimized "production runs." We have used effective values of t_a, t_m, and t_s derived from the experience of Dr. Steve Orszag on the CDC 7600 computer where he has taken care to reduce the run time by optimization and the use of many assembly-language-coded subroutines. The finite-difference method of . Chester Grosch has never been optimized for the 7600, so the figures below are in a sense a rough projection of what the finite-difference method could do if optimized in a similar fashion. Spectral methods are thought to give better resolution of the hydrodynamic variables for a given mesh size. Thus, for calculations of a given accuracy, the number of mesh points required could be less for the spectral

method. Finally, the algorithm for the finite-difference method has been examined in more detail than has that for the spectral method. Given these uncertainties, one should regard the estimates below as only rough indications of the range of computing time required, and not as a comparison of the two methods.

For problems of interest the numbers of mesh points required in the x, y, and z directions fall in the following ranges: L ~ 128-256, M ~ 32-64, and N ~ 8-16. In Table 2 we have estimated the run times for maximum (~ 250,000 mesh points), minimum (~ 33,000), and typical (~ 66,000) problems. ΔT, the computer time per calculation time step is calculated from Eqs. (8) and (9) using "effective" values of $t_a \sim 130$ ns, $t_m \sim 260$ ns, and $t_s \sim 1$ μs. These effective values are derived from the experience of Dr. Steve Orszag on the CDC 7600 computer, but we have used them for estimating both ΔT_s and ΔT_{fd}. Typically, 300 to 500 time steps are required to carry a calculation to the transition stage, so we have taken $T = 400\ \Delta T$ as the total run time.

Table 2

ESTIMATED COMPUTING TIME FOR SPECTRAL AND FINITE-DIFFERENCE METHODS

Problem	L	M	N	LMN	ΔT_{fd}	ΔT_s	T_{fd}	T_s
Maximum	256	64	16	262,144	20 s	40 s	2.0 hr	4.0 hr
Minimum	128	32	8	32,768	2 s	4 s	0.2 hr	0.5 hr
Typical	128	64	8	65,536	5 s	8 s	0.5 hr	0.9 hr

Note: L = Along flow; M = Normal to flow; N = Along span.

Again we should emphasize that these figures should not be taken as a comparison of the finite-difference and spectral methods--they are too rough. The main point here is that for suitably optimized codes the run times are not unacceptably long. Given a typical cost of ~ $700 per hour for a 7600, the production run cost for the "typical" problem is about $500. Optimization and assembly language coding (assumed here), which take advantage of the architecture of a given computer, can give a time reduction as large as a factor of five. So one could expect an unoptimized run to cost about two to five times as much as these "production runs."

IV WAKE OF A FLAT PLATE

A problem closely related to the above transition in the boundary layer of a flat plate is that of transition in the wake of a flat plate. Some reasons for considering this problem next are:

(1) The calculations are very similar to the previous one. A suitable program for the flat-plate calculation would require modest changes in order to treat the wake.

(2) Detailed experimental information is available for comparison (for example, see Sato and Kuriki, 1961).

(3) The nature of the transition is rather gentle. In contrast to many other turbulent transitions, this one is not achieved by the development of sharp bursts. Accordingly, it may be expected that transition can be followed numerically very far.

Drawbacks to this calculation are:

(1) As previously, the downstream boundary conditions are ambiguous.

(2) The applications to practical design are somewhat indirect.

Our understanding of this transition runs as follows: The Goldstein (laminar) wake (Goldstein, 1933) is unstable according to two-dimensional linear stability theory. Thus a small perturbation is amplified when one proceeds downstream. Eventually nonlinear effects take over. (The growth rate is not the predicted exponential, and harmonics of the induced perturbations appear.) Further downstream a distinct three-dimensional pattern appears and the flow becomes more and more irregular. However, we emphasize that no sharp bursts or spikes appear. This should be an ideal problem for numerical simulation.

Preceding page blank

Since, as indicated, the problem is so much like the flat-plate transition, computing requirements will also be pretty much the same.

V WEDGE FLOWS

The numerical simulation of transition in wedge flows would be of considerable interest. The reasons for this are:

(1) The calculation is very similar to the flat plate. [Indeed, one code (Grosch, 1974) has been written to include this possibility.] The essential reason for this is that the boundary-layer equations for the flat plate are just a special case of that for the wedge. Thus, if $\beta\pi$ is the included angle, the potential flow is

$$U(x) = U_o x^m \quad , \tag{10}$$

where

$$m = \beta/(2 - \beta) \quad ,$$

and the boundary layer is described by the equations (Schlichting, 1960, p. 143):

$$u = U_o x^m f'(\eta) \quad , \quad v = -\sqrt{\frac{m+1}{2}\nu U_o x^{m-1}}\left\{f + \frac{m-1}{m+1} f'\right\} \quad , \tag{11}$$

$$\eta = y\sqrt{\frac{m+1}{2}\frac{U_o}{\nu}} x \frac{m-1}{2} \quad , \tag{12}$$

$$f''' + ff'' + \beta[1 - (f')^2] = 0 \quad , \tag{13}$$

subject to $f(0) = f'(0) = 0$, $f'(\infty) = 1$.

We note that with $\beta = 0$ this is just our flat-plate equation. (The factor-of-2 difference occurring between Eqs. (5) and (13) is due to a different normalization.)

(2) By varying the parameter β we can study the effects of pressure gradient. Thus, with $\beta > 0$ we have accelerated flow (and therefore greater stability), while for $\beta < 0$ we have deceleration (and more instability).

(3) With $\beta = 1/2$ we have the equations of the boundary layer for a rotationally symmetric flow.

(4) Measurements of the boundary-layer transition on a flat plate with mild, favorable pressure gradients (DeMetz, 1974) are available for comparison with the calculations.

As we have indicated, the computing requirements are as for the flat-plate case.

VI POSSIBLE FUTURE PROBLEMS

There seem to be many different mechanisms for transition to turbulence. For an understanding of these mechanisms, it would be desirable to do numerical simulation in relatively pure situations. Here we give a list of some of these and an indication of why they are of interest. (Since the calculations are of a somewhat different nature than those described above and have less direct practical application, we think they should be done at some later date. Accordingly, we have not made any computing estimates. However, it seems that they are problems of a magnitude similar to that of the problems discussed above--but computation would probably require new codes.)

A. Couette Flow

This flow between concentric rotating cylinders is, of course, classic. Extremely good experimental results are available (Donnelly, 1963; Coles, 1965). From a theoretical standpoint this is a very clean problem. The ambiguity of the boundary conditions disappears. In the radial direction we have well defined boundary conditions on the cylinders. Azimuthally we have periodicity. In the longitudinal direction periodicity is a reasonable requirement.

When the inner cylinder rotates more rapidly, there is seen experimentally a rich set of phenomena (Coles, 1965). When the rotation rates are changed we pass from the original laminar state through a multitude of different states with well organized flow patterns. In addition, hysteresis effects manifest themselves--i.e., the state achieved depends on the past history. It would be fascinating to reproduce these effects by numerical simulation and it should be possible to do so.

When the outer cylinder rotates more rapidly, something that Coles (1965) has called "catastrophic transition" occurs. There is a sudden jump to states with significant turbulence. Frequently there are alternate spirals of turbulent and laminar fluid. This could well be not resolvable with present computers.

B. The Bénard Problem

This is the problem of a fluid heated from below. Mathematically it is closely related to the Couette flow. Linear stability theory correctly predicts the change from the quiescent state. However, it makes no prediction as to the structure that develops--hexagonal cells, rolls, etc. Model-type calculations--essentially including some nonlinearity--have been done to determine the structure. Since these calculations are quite similar to those made to describe the nonlinear region in transitions on a flat plate, it would be worthwhile to see with numerical simulations how good these calculations are.

C. Poiseuille Flow

1. Between Parallel Planes

The results of linear stability theory (Figure 7) for this flow are strikingly similar to those for the flow over the flat plate. Accordingly, it may be expected that transition to turbulence will occur as in the case of the flat plate. One major advantage is that the downstream boundary-condition problem can be avoided by the reasonable assumption of periodicity. A disadvantage compared to the flat-plate case is that comparable detailed experimental information does not seem to be available.

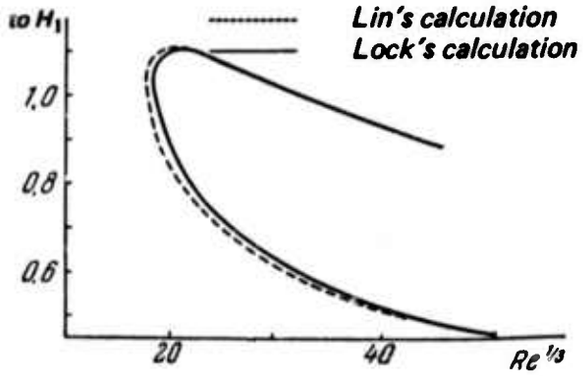

FIGURE 7 THE FORM OF THE NEUTRAL CURVE IN THE (k,Re) PLANE FOR A PLANE POISEUILLE FLOW. Source: Monin and Yaglom (1971).

2. In Pipes

This is a particularly interesting situation since, in contrast to all other problems we have discussed, the flow is apparently stable with respect to infinitesimal disturbances. We say apparently since:

(1) Extensive theoretical efforts using linear-stability theory have failed to find any unstable modes.

(2) Experimentally the transition Reynolds' number seems to go ever higher, the lower the ambient disturbance level. (Of course, neither of these is a proof.)

At least two ideas as to how the observed turbulence originates have been suggested. One is that there is a finite amplitude instability. If this is the case, numerical simulation seems to be of little value. The observed transition in terms of turbulent bursts suggests that in a calculation we would either be in a laminar region (of little interest), or in a turbulent region where we cannot resolve the flow. The second suggestion (Smith. 1960) is that turbulence originates in the inlet region before the full Poiseuille profile develops. If this picture is correct, the numerical calculations would be similar to those for the

flat-plate boundary layer. It should be possible to calculate most of the way to transition to fully developed turbulence.

D. Modifications of the Flat-Plate Problem

Assuming successful completion of the flat-plate calculations, a number of interesting numerical experiments might be performed. Some require very little code modification. Thus, the effects of suction, roughness, and compliant boundaries can be treated by merely changing the boundary conditions imposed on the plate. The effects due to heating could also be treated. An additional equation (for the temperature) would have to be used, and the appropriate variation in viscosity needs to be included. While some recoding would be necessary, the order of magnitude of the computation needed would not be changed.

VII ON CONTROLLING THE TRANSITION TO TURBULENCE

The development of a three-dimensional numerical simulation code will give us a powerful new tool for assessing methods to control the transition to turbulence on a wide range of bodies--i.e., not just bodies of revolution and two-dimensional airfoils. We use the phrase "controlling the transition" in a general sense so that studies of effects that substantially advance the transition (e.g., excessive surface roughness) are also included in the scope of the investigations.

Let us first turn to ways to calculate and control linear Tollmein-Schlichting instabilities. Here a number of methods have already been suggested: (1) compliant surfaces, (2) changing the equation at state (e.g., adding heat, polymers, etc.), (3) suction, and (4) control of the pressure gradient. Except for pressure gradients, which have enjoyed wide use, the optimum ways to use Methods 1 through 3 remain to be devised. Furthermore, even though one is dealing with linear-stability problems, there are important nonlinear effects in the ways the laminar boundary layer and potential flow patterns are altered by the measures used to delay the transition. For example, adding heat changes the viscosity, and the viscosity gradient in turn alters the laminar boundary layer in a direction toward stability. Clearly, heat added at one location on the surface of a body will diffuse across the boundary layer and have a much smaller effect downstream. Thus the combination of heat transport via diffusion and convection, coupled with the linear-instability mechanisms, becomes a complicated problem that is probably most easily solved by a direct simulation rather than linear-stability analysis. The present codes must be generalized to include heat transport, of course.

The second-class methods to alter the transition involve nonlinear changes in the flow within the boundary layer--e.g., nonparallel flows, surface roughness, and abrupt changes in the body shape. As examples we can cite the early transition to turbulence that occurs on some rough, blunt bodies and the use of small span-wise or flow-wise grooves to stabilize the Tollmein-Schlichting waves. Also, swept-wing airfoils have boundary layers with nonparallel flow. The numerical simulation approach gives us a single technique that can handle this wide variety of problems.

Overall, our studies indicate that numerical simulation techniques have sufficient resolution to accurately predict transition and that they can be adopted to circumstances where the laminar boundary layers differ appreciably from the simple parallel-flow ones now commonly used. Initial studies of such phenomena would take a year to complete, and a comprehensive program would require three to five years.

VIII THE IMPACT OF NUMERICAL SIMULATION OF TURBULENCE

Let us suppose that three-dimensional numerical simulation techniques have successfully reproduced many of the phenomena that occur in flat-plate flows. What comprises the next generation of problems both in the practical and research areas?

An important class of practical problems concerns the simulation of the transition to turbulence in configurations where linear-stability analysis fails or is excessively complicated due to geometry. These problems will require the development of a more flexible code that can handle both fairly general boundary conditions (e.g., surfaces rough on the scale of the boundary layer) and heat transport. Fortunately, almost every body can be represented by a sequence of simulations each of which represents a small portion of the surface.

The impact of the numerical simulation of turbulence is that it will be a single technique that will handle many problems not only of a linear-stability type but also inherently nonlinear, such as finite-amplitude surface roughness. The ability to compute the combined effects of both linear and nonlinear processes for initiating transition is a strength unique to the numerical simulation approach.

The next generation of research problems should be chosen to help us understand how well the simulation code represents fully developed turbulence. Estimates clearly indicate that the inertial range will be described poorly if at all. For example, high-frequency bursts of turbulence may not occur in the correct frequency range. On the other hand, many of the overall properties of a turbulent boundary layer (such as drag, heat transport, etc.) may be quite well represented since they

depend much more on the larger, energy-containing eddies. Therefore, there exists a strong possibility that numerical simulation may produce a useful enough representation of the turbulent boundary layer so that the effect of body shape, etc., on the transport properties of the layer can be calculated--at least in a semi-quantitative manner. Such a program would require codes with flexible boundary conditions and carefully thought out sub-grid closure schemes. Its impact would be to produce a first-principles calculation of the arbitrary coefficients that occur in turbulent-boundary-layer theory, and, more importantly, to see if there are circumstances in which these coefficients vary by a significant amount.

IX RECOMMENDATIONS

A program of numerical simulation that could be expected to have a significant impact on our knowledge of, and ability to predict, the transition from laminar to turbulent flow might consist of the following:

(1) A commitment to the program for a significant length of time. Crash programs seem to be counterproductive. Four to five years is a reasonable time scale.

(2) An aspect of competition. There should be at least two groups performing the calculations. In the beginning they should be calculating as closely as possible the same problem, and with the same parameters used in the experiments. Later, when confidence has been obtained the groups could begin dividing up the problems suggested. It is reasonable that the groups use somewhat different computation schemes. A number of such schemes suggest themselves. It would be efficient to use the program to evaluate their relative merits. The schemes used to date--i.e., those of Grosch and Orszag--seem sufficiently representative.

(3) A small advisory panel. This might consist of a group (~ 4) of active workers in the field. The members might be an experimentalist, a theoretical hydrodynamicist, a computer expert, and a numerical analyst. They would be expected to work closely with the computing groups. Hopefully, they would spot difficulties or uncertainties in given calculations and direct the program (i.e., while we have given a tentative ordering of problems to be done, it would be expected that the advisors would continually reassess the next stages of the program in the light of what had been accomplished).

(4) An expenditure of the order of $200,000 per year. This might produce between 30 and 100 runs on one of the problems outlined above. We envisage a few man-years of effort and computation on a computer comparable to the 7600. This sum may or may not include support for experimental work that might be found advisable.

Appendix A

LINEAR-STABILITY ANALYSIS AS A PRACTICAL TOOL

Preceding page blank

Appendix A

LINEAR-STABILITY ANALYSIS AS A PRACTICAL TOOL

On a properly designed and fabricated body, the transition from laminar to turbulent boundary layers occurs through linear instabilities whereby free-stream fluctuations in velocity, pressure, and temperature enter the boundary layer and are spatially amplified via the Tollmein-Schlichting waves. A sufficiently large amplification results in non-linear effects that initiate the transition to turbulence. The transition prediction method of A.M.O. Smith and his colleagues is the only prediction method that now makes use of the spatial amplification concept--a process that must occur physically. Indeed, Smith's e^{10} method has been the most successful predictor in ARPA's program as well as in predicting transition for the various airfoils.

But Smith's method has not received wide use because the spatial amplification rates are derived from the solution to an eigenvalue problem involving 4th-order differential equations. The solution to these equations, which must be done by computer for an arbitrary laminar boundary layer, are conceptually straightforward but quite laborious in practice. A well documented and widely available computer program is called for.

We therefore recommend that ARPA fund an effort to produce a computer program (most likely in FORTRAN) that will run on a number of the more generally available scientific computers. The core of the program will be the 4th-order eigenvalue solver. Auxiliary parts will integrate the spatial amplification factor along the body, and calculate the laminar boundary layer, potential flow, etc.

Preceding page blank

The wide availability of such a program would allow body designers to test proposed bodies against Smith's criterion on an in-house basis, hopefully allowing a more rapid convergence to optimum designs.

The need for this computer program is an example of a situation in which an increased understanding of the basic physics has led to more sophisticated design criteria that can be implemented only by a computer program. Of course, some generality is lost from the older, more gross engineering criteria. But, it is only through such a program that the effects of the details of body shape on the transition to turbulence can be quickly evaluated.

In closing this section, we should remind the reader that transition can occur through channels other than linear Tollmein-Schlichting amplification. High levels of free-stream turbulence, excessive surface roughness, and poor body fabrication are examples. The spatial amplification method often does not work in such cases. But it does have a good record of success in those projects where designers have taken the trouble to eliminate these other sources of turbulence.

Appendix B

REMARKS ON A SPECIALIZED NAVIER-STOKES COMPUTER

Appendix B

REMARKS ON A SPECIALIZED NAVIER-STOKES COMPUTER

1. Introduction

Reference 2 has considered the question of what can be accomplished with modern machines such as the ILLIAC IV, IBM-370/195, and CDC-7600. The purpose of this appendix is to consider the wisdom of designing a special computer that could greatly exceed the capabilities of the current machines in solving only a specialized class of problems--i.e., the Navier-Stokes equations, and similar partial differential equations arising in plasma physics, hydrodynamics, weather prediction, geology, etc.

a. An Interesting Calculation

An interesting numerical simulation well beyond the capabilities of current machines is the fully resolved three-dimensional turbulent fluid flow for a Reynolds number of 10^4. This requires a grid of $(10^4)^{9/4} = 10^9$ mesh points for each point in time. Each mesh point must represent the velocity and pressure fields so that three velocities and one pressure term are required at least for the present instant in time and the immediate past. The past values are needed in order to march forward in time with a numerical integration procedure. Thus 8×10^9 scalar variables are required, and about $(10^4)^3 \ln 10^4 \cong 10^{13}$ arithmetic operations are required. A more detailed count of arithmetic operations of an efficient finite differencing scheme for 10^9 grid points indicated that 5×10^{11} additions and 3×10^{11} multiplications are needed per time step. A rough guess is that about 10^{12} instructions would be required

Preceding page blank

to implement these operations so that about 2×10^{12} read accesses from storage are required for each simulated time step. These parameters are summarized in Table B-1.

Table B-1

PARAMETERS OF AN INTERESTING TURBULENCE CALCULATION

Three-Dimensional Geometry	
Reynolds number:	$R = 10^4$
Resolution:	10^9 spatial mesh points per time step
Memory size:	10^{10} scaler variables
Arithmetic operations (finite-difference method)	
Additions:	5×10^{11} per time step
Multiplications:	3×10^{11} per time step
Instruction execution rate:	10^{12} per time step
Memory bandwidth:	2×10^{12} read accesses per time step

b. Current General Purpose Computers

Table B-2 lists some critical state-of-the-art parameters of modern computers. Note that with a simple array system of secondary-storage access systems, more than $2 \times 10^{10} \times (2 \times 10^6)^{-1} = 10^4$ s would be required just to update each grid point for each simulated time step. Parallel access to the secondary storage will reduce this time, however. The instruction execution time for a very-high-performance single CPU (control processing unit) is at best 25×10^{-9} s, so that $25 \times 10^9 \times 2 \times 10^{12} = 5 \times 10^4$ s or about 14 hours per simulated time step would be required. Thus it seems infeasible to simulate 10^9 grid points since

Table B-2

MAXIMUM-PERFORMANCE PARAMETERS
FOR A MODERN SINGLE, PIPELINED AND CACHE CPU COMPUTER

Direct-access secondary-storage capacity:	10^{11} bits maximum--i.e., about 2×10^9 variables
Direct-access secondary-storage bandwidth:	10^7 bits/s maximum--i.e., about 2×10^6 variables/s
Arithmetic operation time:	25×10^{-9} s minimum (pipelined)
Cache memory access time:	25×10^{-9} s minimum

many time steps would be required in a practical problem. Clearly, the usual von Neumann computer architecture cannot be used, and other choices should be considered.

c. ILLIAC IV

The ILLIAC IV (Bell and Newell, 1971) is a radical departure from classical computer architecture. It was designed for array-type calculations. The critical parameters of the ILLIAC IV are given in Table B-3. The most limiting factor is the limited secondary storage of only 10^9 bits as compared to the 10^{12} bits that are required. Even if the ILLIAC should be supplemented with large disc drives, the bandwidth to secondary storage would be less than 10^9 bits/s as compared to 60×10^{10} bits needed for one simulated time step. It would take more than $60 \times 10^{-9} = 600$ s just to read in data for one simulated time step. Calculations would require about $2 \times 10^{12} \times 2 \times 240 \times 10^{-9} + 64 = 15{,}000$ s per simulated time step, if all input-output and grid-point data interchanges are ignored. Thus even an extensively enhanced ILLIAC IV cannot be us

Table B-3

ILLIAC IV PARAMETERS

64 processing elements	
Add time (each element):	240 ns
Multiply time (each element):	400 ns
2048-64 words of 240-ns memory/element	
Secondary storage capacity:	10^9 bits
Secondary storage bandwidth:	10^9 bits/s (to all elements in parallel)

to attack this problem, and other types of computer structures need to be examined.

2. Computer Architecture for Array Calculations

a. Solution Methods

Nonlinear partial differential equations can be solved by a variety of techniques such as finite difference, spectral, psuedospectral, and Monte Carlo methods. A special computer designed for any one of these methods will not be optimal for any of the others. Also, while it appears that finite-difference methods are the most flexible relative to boundary complexity, etc., the pseudospectral methods are much better when regular surface boundaries exist. Furthermore, integration algorithms are in a dynamic state of development and better algorithms are quite likely to emerge in the near future. Thus, only very flexible and general computer structures should be considered.

b. Computing Requirements

What are the common characteristics of a large class of nonlinear partial differential equation solution methods? First of all, for very arbitrary boundary conditions some finite-difference and successive over-relaxation methods must be employed. However, if well behaved boundaries (planes, spheres, cylinders, etc.) exist, then the pseudospectral methods offer large savings in computing effort. In fact it appears that the 10^9 grid problem will be attacked in the foreseeable future only by pseudospectral or other methods that take advantage of particular features of a given problem. Finite-difference and relaxation methods require only that information be passed between neighboring grid points. The spectral techniques on the other hand need global information at every grid point in order to calculate a Fourier or other transform (Orszag, 1974). However, a very large class of transforms can be implemented through the fast Fourier transform (FFT). Thus the architecture of the computer should be such that grid points can interchange information with their close neighbors and also be able to perform 3-dimensional FFTs on the quantities of the grid points.

From Table B-1 it is evident that to solve the Navier-Stokes equations, for a large number of grid points, about ten variables per grid and 1000 operations per grid point are required for each simulated time step. More complicated problems involving compressible fluids, electromagnetic fields, etc., might double both of the quantities so that in designing a relatively flexible computer, perhaps 32 variables per grid point should be selected and 2000 to 4000 operations per grid point per time step assumed. If it is desired that a time step be simulated in about a second, then about 3200/32 = 100 operations per second are needed for every variable.

c. Performance Tradeoffs

Very fast pipelined logic (a high-performance processor) could perform about 2×10^7 operations per second while a slow serial processor might only be able to do about 3×10^3 operations per second.

For one second of execution time per simulated time step, $2 \times 10^7/2000 \cong 10^4$ grid points could be processed by a single high-performance processor with (10 to 32) $\times 10^4$ registers per processor (i.e., approximate 10^6 bytes). However, an interconnected array of $10^9 \times 10^4$ or $10^9 \times 10^5$ high-performance processors would be required to handle the 10^9 grid-point problems. This approach seems to be far beyond near-term technology hence is therefore considered infeasible. Even if the calculation time were increased considerably and the logic speeds could be greatly improved, an impossibly large array of very-high-performance computers would still be required. In any case, the processors of such an array would be very similar in structure to the present high-performance machines discussed earlier so that beyond creating special FFT hardware attachments to the usual sort of pipelined processor (or array processors for ILLIAC IV), it appears that little can be gained by a special computer architecture using high-performance operations.

An interesting situation develops, if however, the low-performance serial organization is considered. If one slow serial processor were "devoted" to one grid cell and hence 32 variables, the resulting computer structure would be a three-dimensional array of slow serial processors, each with about 32 registers, connections to its neighbors (six each), and connections to implement an FFT (see Appendix E for duration of the FFT) in three dimensions (six additional connections per cell).

A more efficient arrangement in terms of total number of interconnections is to use one processor for every (N^3) grid points; for the

lowest-speed serial processor, this could require as long as ten seconds to simulate one time step. This may very well be an optimal arrangement for a special-purpose computer devoted to solving hydrodynamic equations. As N is increased, the arrangement of cells is not changed but a few more instructions per cell are required for individual grid-point selection within a given cell. Table B-4 illustrates the possibilities for several values of N. It is significant to note that by 1980, it may be feasible to construct a computer to solve the 10^9 grid problem for about the cost of the ILLIAC IV (in 1970 dollars).

3. Conclusions

It can be concluded that:

(1) Direct numerical simulation of turbulence for most important and interesting problems cannot be accomplished with present-day computers or even with general-purpose computers proposed for the near future. Hence, many of these simulations will be impossible without special-purpose computers that have been custom designed to solve partial differential equations.

(2) Algorithms for solving partial differential equations are in a dynamic state of development. Thus any proposed special-purpose computer must be very flexible relative to solution method as well as to the kinds of problems it can handle. In particular, it should be capable of finite-difference calculations and relaxation calculations as well as spectral and pseudo spectral calculations for sets of partial differential equations that arise in hydrodynamics, plasma physics, aerodynamics, global weather, etc. Hence, each grid point must be able to exchange information with neighboring grid points and must be capable of in-place, three-dimensional fast Fourier transformation of the grid-point quantities.

(3) A special purpose very-high-performance computer could be organized for the 10^9-grid-point problem by using a large-variety of high-performance, expensive components. However, the many different types of components required and their diverse interconnections would not allow any

Table B-4

CELLUAR-ARRAY-COMPUTER PARAMETERS

Number of Grid Points per Processor	Number of Registers per Cell	Number of RAM Bits per Cell	Number of Connections per Cell	Seconds of Execution Time per Time Step	Number of Cells for 10^9 Grid	Comments
$1^3 = 1$	32	1.5K	22	1	10^9	
$2^3 = 8$	256	10K	23	8	$\approx 10^8$	1974 state-of-the-art MOS technology
$3^3 = 27$	1,000	40K	24	27	$\approx 4 \times 10^7$	1974 state-of-the-art production-line CCD technology
$4^3 = 64$	2,000	70K	28	64	$\approx 2 \times 10^7$	
$5^3 = 125$	4,000	$\approx$ 100K	29	125	10^7	
$6^3 = 216$	6,000	$\approx$ 200K	30	216	5×10^6	Lab demonstration and state-of-the-art CCD technology
$7^3 = 343$	10,000	$\approx$ 300K	31	343	3×10^6	
$8^3 = 512$	16,000	$\approx$ 500K	32	512	2×10^6	
$9^3 = 729$	20,000	1M	33	729	65×10^6	1980 estimated production state of art
$10^3 = 10^3$	32,000	1.5M	32	1000	10^6	1980 estimated best lab demonstration of state of the art

regular construction pattern, so that the complexity would be overwhelmingly great. Such a machine appears impractical for the near future (the next 10 to 15 years).

(4) A cellular-array computer, composed of a single inexpensive general-purpose minicomputer driving a very large, regular array of identical cells of a single type, each cell of which represents one or more grid points, does appear to be feasible for the 10^9-grid-point problem by the early 1980s.

(5) A cellular array of more modest size might be very effective for calculating some specialized problems in the transition to turbulence, plasma instability, etc. Hence, some smaller array may be worthwhile prior to the 1980s, when ISF technological advancements will probably allow the construction of the large array for a cost that is not totally unreasonable.

(6) A very modest investigation of the cellular-array computer appears to be justified, since many interesting questions must be answered before such a machine could be constructed.

(7) Extensive simulation of the array machine should precede any commitment to hardware. This could be accomplished by a continuing research program at modest cost.

(8) The potential benefits of a powerful computer of the type proposed here seem to be very great. Some further investigation is certainly indicated.

Appendix C

A MODEL TO STUDY DOWNSTREAM BOUNDARY CONDITIONS

Preceding page blank

Appendix C

A MODEL TO STUDY DOWNSTREAM BOUNDARY CONDITIONS

In the main text a number of arguments were given to suggest that downstream boundary conditions cause little effect at a few-boundary-layer thickness upstream. Here we give a simple model in which we can verify the statements.

We consider Couette flow between a stationary plate at $y = 0$ and a plate moving with velocity U in the x-direction at position $y = \delta$. The laminar solution of the Navier-Stokes equations is

$$\underset{\sim}{v} = \left[u_o(y),\ 0,\ 0\right] \quad , \quad \text{where } u_o(y) = Uy/\delta \quad .$$

(Thus we are approximating the Blasius-type profile by a straight line.) Further, we neglect viscosity and restrict ourselves to flow linearized around the laminar solution. We wish to see how a disturbance at a point affects the flow upstream and downstream from that point. Writing $\underset{\sim}{v} = (u_o + u_1,\ v_1,\ 0)$ we have the equations

$$\frac{\partial u_1}{\partial t} + u_o \frac{\partial u_1}{\partial x} + v_1 \frac{\partial u_o}{\partial y} = -\frac{\partial P_1}{\partial y}$$

$$\frac{\partial v_1}{\partial t} + u_o \frac{\partial u_1}{\partial x} = -\partial P_1/\partial y$$

$$\frac{\partial u_1}{\partial x} + \frac{\partial v_1}{\partial y} = 0 \quad .$$

Introducing a stream function φ by

Preceding page blank

$$u_1 = \frac{\partial \varphi}{\partial y} \quad , \quad v_1 = -\frac{\partial \varphi}{\partial x}$$

we readily find that

$$\left(\frac{\partial}{\partial t} + u_o \frac{\partial}{\partial x}\right)\left(\frac{\partial^2 \varphi}{\partial x^2} + \frac{\partial^2 \varphi}{\partial yz}\right) = 0 \quad .$$

(Note that $\partial^2\varphi/\partial x^2 + \partial^2\varphi/\partial y^2$ is just the vorticity of the perturbed flow.) Taking ordinary Fourier transforms with respect to space and one-sided ones in time--i.e.,

$$\tilde{\varphi}(x,y,\omega) = \int_0^\infty e^{i\omega t}\, \varphi(x,y,t)\, dt \quad ,$$

and

$$\approx{\varphi}(k,y,\omega) = \int_{-\infty}^{\infty} e^{-ikx}\, \tilde{\varphi}(x,y,\omega)\, dx$$

--we see that

$$\frac{d^2 \approx{\varphi}}{dy^2} - k^2 \approx{\varphi} = \frac{\tilde{W}(k,y,0)}{i(ku_o - \omega)} \quad , \qquad \text{(C-1)}$$

where $\tilde{W}(k,y,0)$ is the spatial Fourier transform of the initial value of the vorticity.

Explicitly,

$$\tilde{W}(k,y,0) = \int_{-\infty}^{\infty} e^{-ikx}\, \Delta\varphi(x,y,0)\, dk \quad .$$

If we introduce the Green's function $G(y,y',k)$ by

$$G(y,y',k) = -\frac{\sin ky \sin k(\delta - y)}{k \sin k\delta} \qquad y \le y'$$

$$= -\frac{\sin ky' \sin k(\delta - y)}{k \sin k\delta} \qquad y \ge y'$$

the solution of Eq. (C-1) is given by:

$$\tilde{\tilde{\varphi}}(k,y,\omega) = \int_0^1 G(y,y',k)\, \frac{\tilde{W}(k,y',0)}{i(ku_o(y')-\omega)}\, dy' \quad .$$

Inverting the time Fourier transform gives

$$\tilde{\varphi}(k,y,t) = \int_0^1 e^{-iku_o(y')t}\, G(y,y',k)\, \tilde{W}(k,y',0)\, dy'$$

and then

$$\varphi(x,y,t) = \int_0^1 dy' \int_{-\infty}^{\infty} e^{ik[x-u_o(y')t]}\, G(y,y',k)\, \tilde{W}(k,y'0)\, dk \quad . \qquad \text{(C-2)}$$

Now, let us consider the effect of an initial disturbance at $x = 0$, $y = y_o$. Thus,

$$\Delta\varphi(x,y,0) = \delta(x)\, \delta(y - y_o) \quad .$$

Then $\tilde{W}(k,y',0) = \delta(y - y_o)$ and Eq. (C-2) becomes

$$\varphi(x,y,t) = \frac{1}{2\pi} \int_{-\infty}^{\infty} e^{ik[x-u_o(y_o)t]}\, G(y,y_o,k)\, dk \quad .$$

The integral can now be evaluated by residues. (To avoid unnecessary repetition we report merely the results for $y < y_o$.) Thus,

(a) Consider $x - u_o(y_o)\, t < 0$.

(This includes all upstream points and downstream points after a sufficiently long time.)

The result is:

$$\varphi(x,y,t) = \sum_{n=1}^{\infty} e^{n\pi/\delta\,[x-u_o(y_o)t]}\, \frac{(-1)^n}{n\pi}\, \sin\frac{n\pi y}{\delta}\, \sin\frac{n\pi(\delta - y_o)}{\delta} \quad . \tag{C-3}$$

Notice that the disturbance falls off exponentially with distance upstream (in a length $\sim \delta$) and decreases with time exponentially at any fixed point.

(b) $x - u_o(y_o)\, t > 0$.

These are downstream points at sufficiently small times. Here:

$$\varphi(x,y,t) = \sum_{n=1}^{\infty} e^{-n\pi/\delta\,[x-u_o(y_o)t]}\, \frac{(-1)^n}{n\pi}\, \sin\frac{n\pi y}{\delta}\, \sin\frac{n\pi(\delta - y_o)}{\delta} \quad . \tag{C-4}$$

Thus at a fixed point upstream the disturbance grows [according to Eq. (C-4)], reaches a maximum, and then decreases according to Eq. (C-3).

Appendix D

BOUNDARY CONDITIONS

Appendix D

BOUNDARY CONDITIONS

There is a general class of problems, of which the transition problem is an example, that require a careful examination of boundary conditions. We first examine the question of what must be specified in order to arrive at a unique solution, and we then examine a set of boundary conditions for the specific problem under consideration. Lastly, we show that in principle there is a computational scheme that follows from this specification.

The Navier-Stokes equations for an incompressible fluid governing two flows v_1 and v_2 are:

$$\frac{\partial \underset{\sim}{v}_{1,2}}{\partial t} + \underset{\sim}{v}_{1,2} \cdot \nabla \underset{\sim}{v}_{1,2} = -\nabla P_{1,2} + \nu \nabla^2 \underset{\sim}{v}_{1,2}$$

$$\nabla \cdot \underset{\sim}{v}_{1,2} = 0 \quad .$$

Defining

$$\underset{\sim}{v} = \underset{\sim}{v}_1 - \underset{\sim}{v}_2$$

$$P = P_1 - P_2$$

We find

$$\frac{\partial \underset{\sim}{v}}{\partial t} + \underset{\sim}{v}_1 \cdot \nabla \underset{\sim}{v}_1 - \underset{\sim}{v}_2 \cdot \nabla \underset{\sim}{v}_2 = -\nabla P + \nu \nabla^2 \underset{\sim}{v}$$

Preceding page blank

$$\nabla \cdot \underset{\sim}{v} = 0$$

$$\underset{\sim}{v}_1 \cdot \nabla \underset{\sim}{v}_1 - \underset{\sim}{v}_2 \cdot \nabla \underset{\sim}{v}_2 = \underset{\sim}{v}_1 \cdot \nabla (\underset{\sim}{v} + \underset{\sim}{v}_2) - \underset{\sim}{v}_2 \cdot \nabla \underset{\sim}{v}_2 = \underset{\sim}{v}_1 \cdot \nabla \underset{\sim}{v} + \underset{\sim}{v} \cdot \nabla \underset{\sim}{v}_2 \quad .$$

Thus,

$$\frac{\partial \underset{\sim}{v}}{\partial t} + \underset{\sim}{v}_1 \cdot \nabla \underset{\sim}{v} + \underset{\sim}{v} \cdot \nabla \underset{\sim}{v}_2 = -\nabla P + \nu \nabla^2 \underset{\sim}{v}$$

$$\nabla \cdot \underset{\sim}{v} = 0 \quad .$$

The energy in the difference flow,

$$E = \int \frac{1}{2} v^2 \, dt$$

is governed by

$$\frac{\partial E}{\partial t} + \int \left(\nabla \cdot \underset{\sim}{v}_1 \frac{v^2}{2} + \underset{\sim}{v} \cdot \nabla \underset{\sim}{v}_2 \cdot \underset{\sim}{v} \right) dt = -\int \nabla \cdot P \underset{\sim}{v} + \nu \int \nabla \cdot \nabla \underset{\sim}{v} \cdot \underset{\sim}{v}$$

which may be rewritten

$$\frac{\partial E}{\partial t} = -\int \left(\underset{\sim}{v} \cdot \nabla \underset{\sim}{v}_2 \cdot \underset{\sim}{v} + \nu \frac{\partial v_i}{\partial x_j} \frac{\partial v_i}{\partial x_j} \right)$$

$$- \int ds \left(P \underset{\sim}{n} \cdot \underset{\sim}{v} - \nu \underset{\sim}{n} \cdot \nabla \frac{v^2}{2} + \underset{\sim}{n} \cdot \underset{\sim}{v}_1 \frac{v^2}{2} \right) \quad .$$

If we suppose that $v_1 = v_2$ on the boundaries, the surface terms vanish. Assume that ∇v_2 is bounded and its maximum is given by

$$M = \max(\nabla v_2) \quad .$$

Then

$$\frac{\partial E}{\partial t} \leq 2M(t)E \quad .$$

We can then write

$$0 \leq E(t) \leq E(0)e^{2\int_0^t M(t')dt'}$$

from which it follows that if $E(0) = 0$, $E(t)$ also vanishes.

We have therefore proved that specifying the velocity on the boundaries is enough to provide a unique solution.

We next turn to examine the specification of the boundary conditions appropriate to the problem at hand. The coordinate system is shown in Figure D-1. The steady flow satisfies the exact equations

$$v_x \frac{\partial v_x}{\partial x} + v_z \frac{\partial v_z}{\partial z} = -\frac{\partial P}{\partial x} + \nu\left(\frac{\partial^2 v_x}{\partial x^2} + \frac{\partial^2 v_x}{\partial z^2}\right)$$

$$v_x \frac{\partial v_z}{\partial x} + v_z \frac{\partial v_z}{\partial z} = -\frac{\partial P}{\partial z} + \nu\left(\frac{\partial^2 v_z}{\partial x^2} + \frac{\partial^2 v_z}{\partial z^2}\right)$$

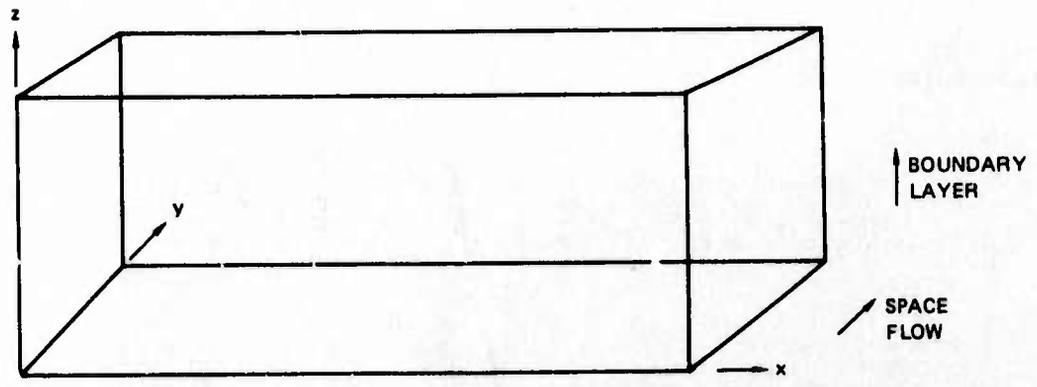

FIGURE D-1 COORDINATE SYSTEM

$$\frac{\partial v_x}{\partial x} + \frac{\partial v_z}{\partial z} = 0 \quad .$$

The usual physical picture of boundary-layer theory involves the assumption that the flow is more slowly varying in the x direction than in the z direction. Thus we may write

$$\frac{\partial}{\partial x} = \epsilon \frac{\partial}{\partial \epsilon x} \qquad \epsilon \ll 1$$

and find

$$v_x \frac{\partial v_x}{\partial \epsilon x} \epsilon + v_z \frac{\partial v_x}{\partial z} = - \frac{\partial P}{\partial \epsilon x} \epsilon + \nu \left(\frac{\partial^2 v_x}{\partial (\epsilon x)^2} \epsilon^2 + \frac{\partial^2 v_x}{\partial z^2} \right)$$

$$v_z \frac{\partial v_z}{\partial \epsilon x} \epsilon + v_z \frac{\partial v_z}{\partial z} = - \frac{\partial P}{\partial z} + \nu \left(\frac{\partial^2 v_z}{\partial (\epsilon x)^2} \epsilon + \frac{\partial^2 v_z}{\partial z^2} \right)$$

$$\frac{\partial v_x}{\partial \epsilon x} \epsilon + \frac{\partial v_z}{\partial z} = 0 \quad .$$

The divergence equation clearly requires

$$v_z = \epsilon \bar{v}_z$$

which yields

$$v_x \frac{\partial v_x}{\partial \epsilon x} + \bar{v}_z \frac{\partial v_x}{\partial z} = - \frac{\partial P}{\partial \epsilon x} + \nu \left(\frac{\partial^2 v_x}{\partial (\epsilon x)^2} \epsilon + \frac{1}{\epsilon} \frac{\partial^2 v_x}{\partial z^2} \right)$$

$$v_x \frac{\partial \bar{v}_z}{\partial \epsilon x} + \bar{v}_z \frac{\partial \bar{v}_z}{\partial z} = - \frac{\partial P}{\partial z} \frac{1}{\epsilon^2} + \nu \left(\frac{\partial^2 \bar{v}_z}{\partial (\epsilon x)^2} \epsilon + \frac{1}{\epsilon} \frac{\partial^2 \bar{v}_z}{\partial z^2} \right) \quad .$$

In order to balance the viscous and inertial forces we then must have

$$v = \bar{v}\epsilon$$

which finally yields the standard boundary-layer equations, which we rewrite in the original variables

$$\frac{\partial P}{\partial z} = 0$$

$$v_x \frac{\partial v_x}{\partial x} + v_z \frac{\partial v_x}{\partial z} = - \frac{\partial P}{\partial x} + \nu \frac{\partial^2 v_x}{\partial z^2}$$

$$v_x \frac{\partial v_z}{\partial x} + v_z \frac{\partial v_z}{\partial z} = \nu \frac{\partial^2 v_z}{\partial z^2}$$

$$\frac{\partial v_x}{\partial x} + \frac{\partial v_z}{\partial z} = 0 \quad .$$

Estimating the terms yields

$$v_x \frac{\partial v_x}{\partial x} \sim \nu_x \frac{\partial^2 v_x}{\partial z^2}$$

or

$$v_x \sim \frac{\nu_x}{z^2}$$

$$v_z \sim \frac{\nu}{z} \quad .$$

This immediately suggests the Blasius similarity solution

$$v_x = Uf(\eta)$$

with

$$\eta = z/\sqrt{\nu x/U}$$

$$v_z = \frac{\nu}{z} g(\eta) \quad .$$

This leads to the nonlinear equation

$$ff'' + 2f''' = 0$$

and the boundary conditions

$$f = 0 \quad , \quad f' = 0 \quad , \quad z = 0$$

$$f' = 1 \quad z \to \infty \quad .$$

Since these solutions are only approximate, part of the flow field that develops in time in the computation will result from the equation trying to predict the actual solutions. We look for solutions of the form

$$f = f(z)e^{-i\omega t} e^{i\beta y} e^{i\int \alpha(x)dx}$$

and we know that the resulting equation is a form of the Orr-Sommerfeld equation which is fourth-order in z. Two boundary conditions are provided by the vanishing of the perturbed flow at the bottom and top, and two more involving the derivatives are provided by the vanishing of other components of the velocity. The resulting eigenvalue equation

$$h(\omega,\beta,\alpha,R) = 0$$

yields the local spatial growth. In general, defining the boundary-layer thickness

$$\delta' \sqrt{\nu x/U}$$

and the Reynolds number

$$R\delta = \frac{U\delta'}{\nu}$$

yields curves of the form given in Figure D-2. The actual experiment of

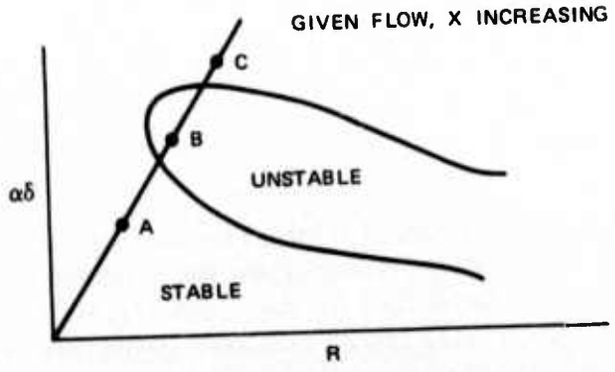

FIGURE D-2 STABILITY DIAGRAM FOR BOUNDARY-LAYER FLOW

Klebanoff et al. (1961) corresponds to point A for the upstream condition. To save calculational time, the numerical calculations may be started at point B, which is 100 cm downstream, and the calculation can be stopped at point C.

A summary of a physically reasonable set of boundary conditions that at least is mathematically unique is then given by

(1) Global constraint, $\int dS\ \underset{\sim}{v} \cdot \underset{\sim}{n} = 0$.

(2) Bottom plate, $\underset{\sim}{v} = 0$, no slip condition.

(3) Top of region, $v_x = U(\infty)$, free stream.

(4) Spanwise, the flow is symmetric. Thus, $v_y = 0$ at the sides, and $\partial v_x/\partial y$ and $\partial v_z/\partial y$ both vanish. Although the original uniqueness proof was carried out for specified $\underset{\sim}{v}$, the surface terms vanish except for

$$\int ds\ n\ \nabla \frac{v^2}{z} = \int dx\ dz \left(v_x \frac{\partial v_x}{\partial y} + v_y \frac{\partial v_y}{\partial y} + v_z \frac{\partial v_z}{\partial y} \right)$$

which vanishes for the specification of derivatives given above.

(5) Upstream. As discussed above, the conditions are

$$v_x = U(z) + \delta v_x$$

$$v_y = \delta v_y$$

$$v_z = \delta v_z$$

where U(z) is the Blasius profile corresponding to a position 100 cm downstream from the entrance, and $\delta \underset{\sim}{v}$ is a linear combination of two- and three-dimensional Tollmien-Schlichting waves. These waves are chosen to correspond to the driving frequency of the ribbon in the Klebanoff experiment and to have the periodicity in y imposed by the spacers.

(6) Downstream. Here we assume that the conditions imposed in (5) are simply carried downstream to a location at $x = L$ corresponding to point C in the stability diagram. We know that the spatial growth is converted downstream with a velocity c that is less then U_∞. Thus, for some period of time, chosen so that transition occurs in the volume of the calculational domain, the downstream boundary conditions will not change.

We now wish to show that, in principle, the specification given above yields a method of numerical calculation. At $t = 0$, the velocity field is specified everywhere and for all t, $\underset{\sim}{v}$ is specified on the boundary.

From the Navier-Stokes equations and $\nabla \cdot \underset{\sim}{v} = 0$, it follows that

$$\nabla^2 P = -\nabla \cdot \left(\underset{\sim}{v} \cdot \nabla \underset{\sim}{v}\right) \quad .$$

A Greens function G satisfying

$$\nabla^2 G = -\delta(\underset{\sim}{x} - \underset{\sim}{x}')$$

yields the solution

$$P = \int ds \ (G\underset{\sim}{n} \cdot \nabla P - P\underset{\sim}{n} \cdot \nabla G) - \int G\nabla \cdot (\underset{\sim}{v} \cdot \nabla \underset{\sim}{v}) \ ds \quad .$$

Since P is unknown on the boundary, choose $\underset{\sim}{n} \cdot \nabla G = 0$ there. We are guaranteed then that G exists. From the normal component of the Navier-Stokes equation on the surface

$$\frac{\partial}{\partial t} \underset{\sim}{v} \cdot \underset{\sim}{n} + \underset{\sim}{v} \cdot \nabla \underset{\sim}{v} \cdot \underset{\sim}{n} = -\underset{\sim}{n} \cdot \nabla P + \nu \nabla^2 \underset{\sim}{v} \cdot \underset{\sim}{n}$$

we see that $\underset{\sim}{n} \cdot \nabla P$ is determined in terms of known quantities. Thus,

$$P = \int G\left[\nu \nabla^2 \underset{\sim}{v} \cdot \underset{\sim}{n} - \frac{\partial}{\partial t} \underset{\sim}{v} \cdot \underset{\sim}{n} - \underset{\sim}{v} \cdot \nabla \underset{\sim}{v} \cdot \underset{\sim}{n}\right] ds - \int G(\nabla \cdot \underset{\sim}{v} \cdot \nabla \underset{\sim}{v}) \ dt$$

and is determined everywhere. Now, knowing P we use

$$\frac{\partial \underset{\sim}{v}}{\partial t} = -\nabla P + \nu \nabla^2 \underset{\sim}{v} - \underset{\sim}{v} \cdot \nabla \underset{\sim}{v}$$

and the knowledge of $\underset{\sim}{v}$ everywhere to advance $\underset{\sim}{v}$ forward in time at every interior point of the calculational mesh. In a crude sense this represents a proof of the existence of solutions to these equations.

Appendix E

THREE-DIMENSIONAL IN-PLACE FAST-FOURIER TRANSFORM ARRAY

Preceding page blank

Appendix F

THREE DIMENSIONAL IN-PLACE FAST-FOURIER-TRANSFORM ARRAY

Assume that it is desired that an array of cells is to be permanently connected with as few connections as possible such that three-dimensional, in-place, fast Fourier transforms can be made of variables stored within the cells. That is, if the elements of matrix A, a_{ijk} are stored in $cell_{ijk}$, then matrix B with elements b_{ijk} are to be calculated according to

$$B = F[A]$$

$$b_{ijk} = \sum_{\ell=0}^{L-1} \sum_{m=0}^{M-1} \sum_{n=0}^{N-1} a_{\ell m} \exp\left[\frac{\sqrt{-1}}{2\pi}\left(\frac{i\ell}{L} + \frac{im}{M} + \frac{kn}{N}\right)\right] .$$

Stone (1970) has shown how a one-dimensional FFT on an array of cells can be accomplished in place by a "perfect shuffle" interconnection between cells. Only two inputs and two outputs per cell are required. Despain (1974) has shown how FFT operations such as those used within the cells used by Stone can be implemented without calculating or storing the trigonometric coefficients usually employed (cordic methods). This makes practical an array of simple identical cells that can be made to perform an in-place transform of variables stored in the cells.

Three-dimensional transforms are generally accomplished as three successive groups of one-dimensional transforms. However, it is possible to simultaneously transform in all three dimensions at the same time. This is of great advantage for the three-dimensional array of cells, since the "perfect shuffle" connections are permanently connected in all three

Preceding page blank

dimensions and parallel data transfer (and calculations too if desired) can proceed simultaneously and at a much greater rate than if separate transforms are taken in succession.

The connection pattern is symmetric in all three dimensions. Figures E-1 and E-2 illustrate these patterns for one and two dimensions.

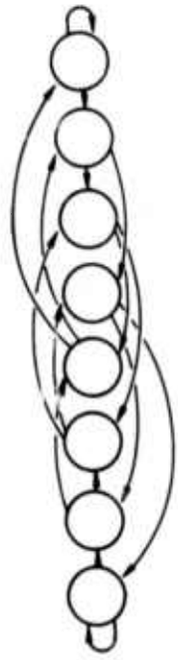

FIGURE E-1 PERFECT SHUFFLE CONNECTIONS FOR 1-D FFT, N = 16

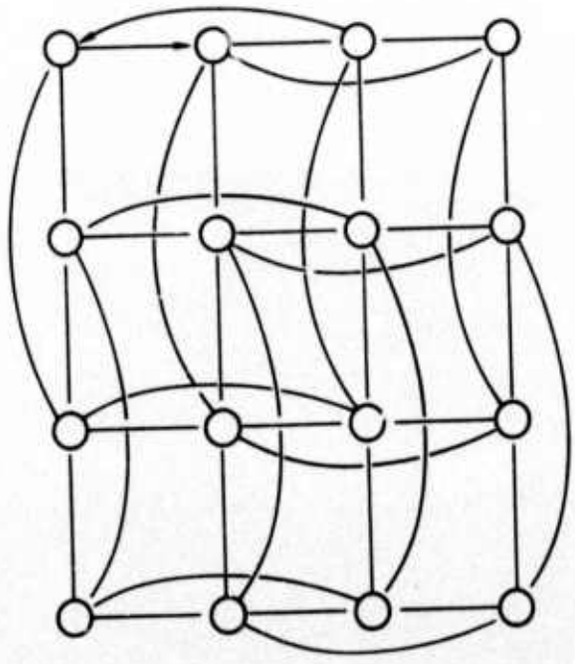

FIGURE E-2 4-BY-4 ARRAY OF CELLS FOR A 2-D FFT NETWORK

REFERENCES

Bell, C. G. and A. Newell, Computer Structures: Readings and Examples (McGraw-Hill Book Co., Inc., N.Y., N.Y., 1971).

Benny, D. J., "A Nonlinear Theory for Oscillations in a Parallel Flow," J. Fluid Mech., Vol. 10, No. 2, p. 209 (1961).

Case, K. M., F. J. Dyson, E. A. Frieman, C. E. Grosch, and F. W. Perkins, "Numerical Simulation of Turbulence," Technical Report JSR-73-3, Stanford Research Institute, Menlo Park, Calif. (1973).

Coles, D., Transition in Circular Couette Flow," J. Fluid Mech., Vol. 21, p. 385 (1965).

DeMetz, F., "Low Speed Boundary-Layer Transition Workshop," July 16, 17, 1974, The Rand Corporation, Santa Monica, Calif.

Despain, A. M., "Fourier Transform Computers Using CORDIC Iterations," IEEE Trans. on Computers, Vol. C-23, No. 10, pp. 993-1001 (October 1974).

Donnelly, R. J., "Experimental Determination of Stability Limits," in Proc. Symp. Appl. Math., Vol. 13, pp. 41-53 (1963).

Goldstein, S., Proc. Roy. Soc. A, Vol. 142, p. 545 (1933).

Greenspan, H. P. and D. J. Benny, "On Shear-Layer Instability, Breakdown, and Transition," J. Fluid Mech., Vol. 15, No. 1, p. 133 (1963).

Grosch, C. E., "Predicting Transition from Laminar to Turbulent Boundary Layer Flow," Report, Old Dominion University Research Foundation, Old Dominion University, Norfolk, Va. (1974).

Klebanoff, P. S., K. D. Tidstrom, and L. M. Sargent, "The Three Dimensional Nature of Boundary-Layer Instability," Fluid Mech., Vol. 12, p. 1 (1961).

Preceding page blank

Kovasznay, L.S.G., H. Komoda, and B. R. Vasudeva, "Detailed Flow Field In Transition," in Proceedings of the 1962 Heat Transfer and Fluid Mechanics Institute, F. E. Ehlers, J. J. Kauzlarich, C. A. Sleicher, Jr., and E. Street, eds. (Stanford U. Press, Stanford, Calif., 1962).

Landau, L. D. and E. M. Lifshitz, Fluid Mechanics, p. 123 (Addison-Wesley Publishing Co., Reading, Mass., 1959).

Lin, C. C. and D. J. Benny, "On the Instability of Shear Flows," Proc. Symp. Appl. Math., Vol. 13, No. 1 (1962).

Monin, A. S. and A. M. Yaglom, Statistical Fluid Mechanics, Vol. 1, p. 130 (M.I.T. Press, Cambridge, Mass., 1971).

Orszag, S. A., "Fourier Series on Spheres," Monthly Weather Review, Vol. 102, No. 1, pp. 56-75 (January 1974).

Orszag, S. A., "Numerical Simulation of Boundary Layer Transition on a Flat Plate," Research Report No. 33, Flow Research Inc., Seattle, Wash. (May 1974).

Sato, H. and K. Kuriki, "The Mechanism of Transition in the Wake of a Thin Flat Plate Placed Parallel to a Uniform Flow," J. Fluid Mech., Vol. 11, p. 321 (1961).

Schlichting, H., Boundary Layer Theory, Chapt. XVI (McGraw-Hill Book Co., Inc., N.Y., N.Y., 1960).

Smith, A.M.O., "Remarks on Transition in a Round Tube," J. Fluid Mech., Vol. 7, p. 565 (1960).

Stone, H. S., "Parallel Processing with the Perfect Shuffle," IEEE Trans. on Computers, Vol. C-20, No. 2, pp. 153-161 (1971).

Stuart, J. T., "On Three-Dimensional Non-Linear Effects in the Stability of Parallel Flow," Advances Aeronaut. Sci., Vol. 3 (Pergamon Press, Oxford, 1962).